

Appendix E

Assessment of Fuel Hydrocarbon Plume Behavior and Biodegradation Rates

Appendix E
Section E-1

**Comparisons of Geochemical Signatures of
Biotransformation of Hydrocarbon in
Groundwater**

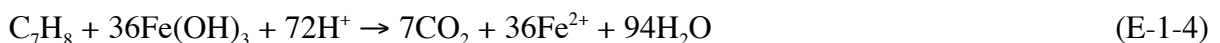
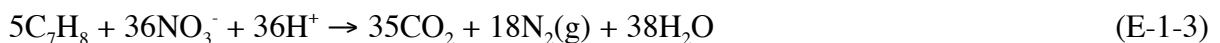
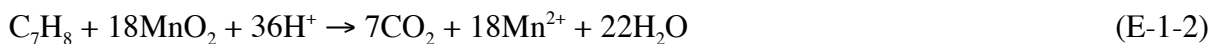
Appendix E (Section E-1)

Comparisons of Geochemical Signatures of Biotransformation of Hydrocarbon in Groundwater

E-1.1. Introduction

Fuel hydrocarbon compounds from leaking tanks and pipelines are common groundwater contaminants. Recently, much interest has developed in utilizing natural attenuation processes to remediate groundwater contaminated with fuel hydrocarbons as opposed to active engineered solutions such as pump-and-treat technology. Natural attenuation includes biotransformation processes which are known from numerous field and laboratory studies to affect fuel hydrocarbons (e.g., Reinhard, Goodman, and Barker, 1984; Barker and others, 1986; Major et al., 1988; Grbic-Galic and Vogel, 1991; Haag et al., 1991; Kazumi et al., 1997). Statistical analyses of large populations of FHC plumes released from leaking underground fuel tanks have shown that fuel hydrocarbon plume lengths are generally limited in extent, presumably as a result of biotransformation processes (Rice et al., 1995; Buscheck et al., 1996; Mace et al., 1997).

Identifying evidence of fuel hydrocarbon biotransformation from field data is a key element in formulating risk management strategies that incorporate natural attenuation at groundwater contamination sites. Primary evidence of biotransformation (i.e., observed decline in total contaminant mass over time) is often difficult to extract from monitoring data because of sparse sampling networks and short sampling histories. Therefore, secondary lines of evidence must often be pursued. Secondary evidence consists of changes in groundwater geochemistry associated with the FHC plume which may reflect the oxidation of fuel hydrocarbons by microorganisms (e.g., Vroblesky and Chapelle, 1994; Borden et al., 1995). For example, the mineralization of toluene, a soluble and biodegradable gasoline constituent, to carbon dioxide could include a number of potential mechanisms:





Laboratory studies have confirmed that fuel hydrocarbons may biotransform through reactions involving a variety of specific electron acceptors (e.g., Lovley et al., 1989; Beller et al., 1992, Lovley et al., 1995; Vroblesky et al., 1996). Groundwater chemical constituents which serve as biotransformation indicators include electron acceptors (dissolved oxygen, nitrate, sulfate), reduced by-products of FHC oxidation reactions (ferrous iron, manganese, methane), solution redox potential or E_h , and indicators of mineralization (bicarbonate alkalinity, pH via dissociation of carbonic acid). Sulfide, also a reduced by-product of fuel hydrocarbon biotransformation, is often not measurable because of the low solubility of sulfide-bearing minerals under the E_h -pH conditions encountered in typical groundwater environments.

Each of these indicator parameters is subject to a certain degree of variability in background concentrations. Given the sparse monitoring well network often associated with fuel hydrocarbon releases, it may often be difficult to discern patterns in spatial distributions of geochemical indicators which offer unequivocal proof of biotransformation. To address this issue, variability in geochemical indicator species has been evaluated from six sites at military bases in California where releases of fuel hydrocarbons to groundwater from leaking underground fuel tanks (LUFTs) have been observed (Table E-1.1). The sites include the Area 43 Gas Station at Camp Pendleton Marine Corps Base (PMCB), the Petroleum, Oils, and Lubricants Fuel Farm Area at Castle Air Force Base (CAFB) near Merced, the Operable Unit 2 area at George Air Force Base (GAFB) near Victorville, the Building 637 area at the Presidio of San Francisco (PSF), the North-South Gas Stations at Travis Air Force Base (TAFB) near Fairfield, and the Base Exchange Service Station at Vandenberg Air Force Base (VAFB) near Lompoc. At each site, total petroleum hydrocarbons (TPH) were measured by gas chromatography. Geochemical indicator parameters were also measured, typically by ion chromatography or atomic adsorption spectroscopy (for ionic species and metals), although not all of the geochemical indicator parameters were available from all the sites. In general, groundwater quality data were available for only two to three years for most of the sites, whereas the likely period of release history spanned many decades as indicated by the site histories.

E-1.2. Analysis

E-1.2.1. Geochemical Evidence of Biotransformation

Consider the hypothetical fuel hydrocarbon plume depicted on Figure E-1.1. As the release occurs, the more soluble components (e.g., benzene, toluene) will dissolve into groundwater and begin to migrate downgradient via advective and dispersive transport. Contemporaneously, indigenous microbiota metabolize the dissolved hydrocarbon constituents for energy and cell mass. As a result, electron acceptors are sequentially depleted in general accordance with the reactions listed in Eqs. E-1-1 through E-1-6. Ideally, the spatial distribution of geochemical indicators would reflect the changes in electron acceptor concentrations, redox conditions, and mineralization associated with the biotransformation reactions. In reality, physical and biogeochemical

heterogeneities, as well as complex boundary conditions, would produce a less coherent distribution of geochemical indicator values. The interpretation of these spatial distributions would also be affected by the limited sampling resolution offered by the monitoring well networks typically installed at LUFT sites. In addition, even if adequate time series data were available, identifying temporal trends indicative of biotransformation would also be problematic in many instances. Because of the release scenarios associated with LUFTs – percolation of light non-aqueous phase liquids (LNAPLs) through the vadose zone to the water table – residual sources of contamination may persist as isolated ganglia or pools of LNAPL even after the LUFTs have been removed. Such sources could continue supplying dissolved-phase hydrocarbons to the aquifer over a period of decades. When coupled with biotransformation processes in the dissolved phase, this scenario may result in a pseudo-steady-state plume, where a dynamic mass balance exists between the influx of dissolved hydrocarbons from residual source dissolution and mass loss via biotransformation. Under this scenario, hydrocarbon concentrations could remain relatively stable over a long period.

Given these issues, one approach for identifying quantitative evidence of biotransformation process from a single sampling event is to compare median values of geochemical indicator parameters from monitoring wells located within the hydrocarbon plume with those which may be delineated as representing background. The use of median values for such a comparison offers the advantage of minimizing the influence of outlier values from either sample set in affecting the interpretation of the data. Differences between median values for a number of geochemical indicators that are consistent with Eqs. E-1-1 through E-1-6 would provide support for a biotransformation hypothesis.

For analyses of geochemical indicator data from the six LUFT sites, monitor wells characterized by detectable quantities of fuel hydrocarbons during the sampling round of interest were designated as plume interior wells. Those wells not exhibiting detectable fuel hydrocarbons were assumed to represent background conditions. Analysis of median concentrations for the geochemical indicator data available from the six LUFT sites strongly supports the assertion that fuel hydrocarbon biotransformation processes are active at each site. Median concentrations of dissolved oxygen (DO) from interior and background wells are shown on Figure E-1.2 for five of the six sites (dissolved oxygen data were not available from the Vandenberg AFB LUFT site). Median dissolved oxygen concentrations from plume interiors are less than the median background concentration at four of the sites. The exception to this pattern, the LUFT site at the Presidio of San Francisco, is located in an anaerobic environment that is rich in natural organic carbon (background DO < 0.5 mg/L). It is likely that under such conditions, reported concentrations of DO would simply reflect atmospheric contamination of the groundwater samples. Median concentrations of nitrate and sulfate are shown on Figures E-1.3 and E-1.4, respectively. These data suggest that both nitrate and sulfate concentrations are depleted within plume interiors compared to background at all six sites, possibly reflecting denitrification and sulfate reduction processes (Eqs. E-1-3 and E-1-5). Median concentrations of ferrous iron and manganese are shown on Figures E-1.5 and E-1.6, respectively; manganese data were not available from the LUFT site at the Camp Pendleton Marine Corps Base. Unlike the geochemical indicators which are aqueous-phase electron acceptors (i.e., DO, NO_3^- , SO_4^{2-}), the concentrations of dissolved iron and manganese become elevated as biotransformation reactions progress. This is because iron and manganese exist as electron acceptors in the solid phase (e.g., as $\text{Fe}(\text{OH})_3$ or MnO_2) under ambient (generally aerobic) conditions. Reduction of these metals from their respective oxidized forms

(Fe^{3+} , Mn^{4+}) to the reduced forms (Fe^{2+} , Mn^{2+}) via Eqs. E-1-2 and E-1-4 results in mobilization and hence increased concentrations.

Median concentrations of dissolved methane are shown on Figure E-1.7. Elevated methane concentrations within the plume interior suggesting methanogenesis are evident at the LUFT sites at Camp Pendleton Marine Corps Base and especially at the Presidio of San Francisco. The strong indication of methanogenesis at the Presidio LUFT site is consistent with the background biogeochemical setting of the site (anaerobic, high natural organic carbon content), particularly given the relatively low concentrations of other electron acceptors such as nitrate and sulfate. Indeed, studies have shown that methanogenesis can become an important mechanism for the transformation of organic compounds if other electron acceptors are depleted (Baedeker et al., 1993; Zhang et al., 1998). Median redox potential (E_h) values are shown on Figure E-1.8. Viewed in isolation, E_h -values may be difficult to interpret because redox reactions are often not in equilibrium and it is difficult to ascertain which specific redox couple is responsible for the observed voltage potential on the E_h -electrode. Nevertheless, E_h measurements are useful as a semi-quantitative guide to the nature of the redox conditions at a particular site. E_h values are clearly lower within the plume interior at each of the sites in comparison to background, with the lowest background values observed at the two sites characterized by methanogenic processes which would be expected only under the most reducing conditions. Thus, observed values of E_h are also consistent with biotransformation (i.e., oxidation) reactions.

Median bicarbonate alkalinity values are shown on Figure E-1.9. Bicarbonate alkalinity is clearly elevated in the plume interiors at each of the sites in comparison to background. A likely explanation for this phenomenon is the dissociation of carbonic acid produced from the mineralization of the fuel hydrocarbons. This hypothesis is supported by the median values of pH observed in interior and background wells (Fig. E-1.10). The production of carbonic acid via mineralization, and the transient presence of trace organic acid intermediate transformation products of the fuel hydrocarbons, would be expected to lower the pH of the groundwater solution, although this would be moderated somewhat by the buffering effects of mineral phases such as calcite. Small differences in median pH values between plume interior wells and background are consistent with such expected pH differences for four of the five sites reporting pH values.

E-1.2.2. Comparison of Geochemical Indicators

The comparison of plume interior and background geochemical parameter values provides semi-quantitative evidence supporting biotransformation processes across several sites. However, in most instances the issue of biotransformation at individual sites will constitute the immediate problem of interest. Again, geochemical indicator parameters may be used to provide semi-quantitative evidence of biotransformation processes. In this case, the problem is one of examining the relationship between geochemical indicator values and hydrocarbon concentrations in individual groundwater samples from a given site.

Rank correlation coefficients describing the relationship between each geochemical indicator parameter and the concentration of TPH for an individual sampling round at each of the six sites are shown on Table E-1.2. Rank correlation was used because of the apparent lognormal distribution of many of the geochemical indicator species concentrations. Four of the parameters, redox potential, ferrous iron, manganese, and dissolved methane exhibit relatively high rank correlations versus TPH, with $r \geq 0.5$ for at least five of the six sites. The remaining parameters

(dissolved oxygen, nitrate, sulfate, pH, and bicarbonate alkalinity) exhibit poorer correlation with TPH overall, with $r \leq 0.5$ for three or more of the six sites. Dissolved oxygen in particular appears to be a poor biotransformation indicator as quantified by correlation with TPH.

For five of the six sites in the study, approximately one-half of the monitoring wells were characterized by TPH concentrations less than the applicable detection limit (i.e., delineated as background wells). As such, the task of identifying meaningful correlations between geochemical indicator parameters and fuel hydrocarbon concentrations becomes more difficult. A logical alternative, therefore, is to divide the sample population for a given indicator into two sets: those associated with detections of TPH and those presumably representing background conditions. The two populations may then be compared using a standard test to ascertain whether or not the means of the two sets differ significantly. The students *t*-test is frequently used for this analysis, although in this case a non-parametric equivalent, the Kruskal-Wallis test, was used instead because of the lognormal distributions of many of the geochemical parameters. The confidence levels pertaining to the significance of differences in the means between the plume interior and background sample sets for each indicator at each site are shown on Table E-1.3 (confidence levels less than 90% were considered to not be significant). In general, these results match those suggested by the correlation analysis: redox potential, ferrous iron, manganese, and dissolved methane concentrations generally differ significantly between the two data sets, whereas oxygen, nitrate, sulfate, pH, and bicarbonate alkalinity often do not. However, these analyses also suggest differences in how the data are distributed at individual sites. For example, most of the indicator parameters at the Travis AFB LUFT site are easily distinguished between the plume interior and background wells, whereas those at the Presidio of San Francisco LUFT site are not. This suggests that patterns of biotransformation are not equally well-delineated between the sites, possibly reflecting spatial heterogeneities in various biogeochemical transformation regimes or differences in how monitoring wells are located relative to the morphology of the plume.

E-1.2. Discussion

Evaluations of the relationships between TPH concentrations and geochemical indicators by both correlation analyses and population means analyses suggest that redox potential, ferrous iron, manganese, and methane are more robust indicators than the other parameters. A likely explanation lies in the difficulty in distinguishing changes in groundwater geochemistry resulting from biotransformation with background fluctuations arising from other causes. In naturally aerobic groundwater settings, ferrous iron, manganese, and methane would be expected to exhibit very low concentrations, whereas those of sulfate and bicarbonate alkalinity may be relatively high. Thus, the biotransformation of small quantities of fuel hydrocarbons may generate a response in ferrous iron that is easily quantified, whereas the utilization of small quantities of sulfate compared to background may go unrecognized.

To test this explanation, a signal-to-noise parameter, Δ , may be defined, in principle, for geochemical indicators (exclusive of E_h and pH) at each site based on median background and median plume interior concentrations:

$$\Delta = \left| \frac{\text{Median } C_{bkg} - \text{Median } C_{plume}}{\text{Median } C_{bkg}} \right| \quad (\text{E-1-7})$$

The ranges of rank correlation coefficients corresponding to the median value of Δ for each parameter at each site are shown on Figure E-1.12. In general, the parameters with Δ -values less than 0 (i.e., parameters with non-zero background concentrations which are depleted in the plume interior by biotransformation processes) exhibit poorer correlation with TPH concentrations than those with positive Δ -values. This is especially true for DO, where background concentrations are relatively low as a result of limited solubility. Because of the difficulty in accurately quantifying DO below approximately 0.5 mg/L in routine groundwater analyses, a very sharp difference between plume interior and background wells may be difficult to observe with relatively few wells overall. On the other hand, background sulfate concentrations are high enough that fuel hydrocarbon biotransformation only depletes a portion of the available sulfate. As a result, variability in background concentrations may match or exceed the concentration loss associated with sulfate reduction. Nitrate represents an intermediate case between oxygen and sulfate. Among the indicators exhibiting positive Δ -values, bicarbonate alkalinity is unique in that significant background concentrations are usually present. As a result, variability in background concentrations tends to reduce the correlation between bicarbonate alkalinity and fuel hydrocarbon concentrations. Correlations with fuel hydrocarbon concentrations are generally the highest with those compounds exhibiting the lowest background concentrations – manganese, methane, and ferrous iron.

The practical utility in these findings is in providing guidance to site investigators as to which geochemical biotransformation indicators are likely to be the most reliable. Future sampling at these sites or longer-term analyses at other sites may assist in confirming the findings. Time series analyses may also provide insights into possible seasonal effects that could influence the interpretation of the data. For example, seasonal changes in rainfall infiltration could alter the ambient groundwater chemistry to the extent that the dominant redox process responsible for biotransformation changes from one electron acceptor to another (e.g., Vroblesky and Chapelle, 1994).

References

- Baedecker, M. J., Cozzarelli, I. M., and Eganhouse, R. P.: 1993, 'Crude oil in a shallow sand and gravel aquifer III. Biogeochemical reactions and mass balance modeling in anoxic groundwater,' *Applied Geochemistry*, **8**, 569–586.
- Barker, J. F., Tessman, J. S., Plotz, P. E. and Reinhard, M.: 1986, 'The organic geochemistry of a sanitary landfill leachate plume,' *Journal of Contaminant Hydrology*, **1**(1/2), 171–189.
- Beller, H. R., Grbic-Galic, D., and Reinhard, M.: 1992, 'Microbial degradation of toluene under sulfate-reducing conditions and the influence of iron on the process,' *Applied and Environmental Microbiology*, **58**, 786–793.
- Borden, R. C., Gomez, C. A., and Becker, M.T.: 1995, 'Geochemical indicators of intrinsic bioremediation,' *Ground Water*, **33**(2), 180–189.
- Buscheck, T. E., Wickland, D. C., and Kuehne, D. L.: 1996, 'Multiple lines of evidence to demonstrate natural attenuation of petroleum hydrocarbons,' in *Proceedings from the Conference on Petroleum Hydrocarbons and Organic Chemicals in Groundwater*, National Ground Water Association/API, Houston, Texas, November 13–15.
- Grbic-Galic, D., and Vogel, T. M.: 1987, 'Transformation of toluene and benzene by mixed methanogenic cultures,' *Applied and Environmental Microbiology*, **53**(2), 254–260.
- Haag, F., Reinhard, M., and McCarty, P. L.: 1991, 'Degradation of toluene and p-xylene in anaerobic microcosms: Evidence for sulfate as a terminal electron acceptor,' *Environmental Toxicology and Chemistry*, **10**(11), 1379–1390.
- Kazumi, J., Caldwell, M. E., Suflita, J. M., Lovley, D. R., and Young, L. Y.: 1997, 'Anaerobic degradation of benzene in diverse anoxic environments,' *Environmental Science and Technology*, **31**(3), 813–818.
- Langley, R.: 1970, *Practical Statistics*, Dover Publications, Inc., New York, New York, 399 p.
- Lovley, D. R., Baedecker, M. J., Lonergan, D. J., Cozzarelli, I. M., Phillips, E. J. P., and Siegel, D. I.: 1989, 'Oxidation of aromatic contaminants coupled to microbial iron reduction,' *Nature*, **339**(5), 297–300.
- Lovley, D. R., Coates, J. D., Woodward, J. C., and Phillips, E. J. P.: 1995, 'Benzene oxidation coupled to sulfate reduction,' *Applied and Environmental Microbiology*, **61**, 953–958.
- Mace, R. E., Fisher, R. S., Welch, D. M., and Parra, S. P.: 1997, 'Extent, Mass, and Duration of Hydrocarbon Petroleum Storage Tank Sites in Texas,' *Bureau of Economic Geology*, University of Texas at Austin.
- Major, D.W., Mayfield, C. I., and Barker, J. F.: 1988, 'Biotransformation of benzene by denitrification in aquifer sand,' *Ground Water*, **26**(1), 8–14.
- Miller, I., and Freund, J. E.: 1977, *Probability and Statistics for Engineers*, Second Edition, Prentice-Hall, Inc., Englewood Cliffs, New Jersey, 529 p.

- Rice, D. W., Grose, R. D., Michaelson, J. C., Dooher, B. P., MacQueen, D. H., Cullen, S. J., Kastenbergh, W. E., Everett, L. E., and Marino, M. A.: 1995, *California Leaking Underground Fuel Tank (LUFT) Historical Case Analyses*, Lawrence Livermore National Laboratory, Livermore, Calif. (UCRL-AR-122207).
- Reinhard, M., Goodman, N. L., and Barker, J. F.: 1984, 'Occurrence and distribution of organic chemicals in two landfill leachate plumes,' *Environmental Science and Technology*, **18**(12), 953–961.
- Vroblecky, D. A., and Chapelle, F. H.: 1994, 'Temporal and spatial changes of terminal electron-accepting processes in a petroleum hydrocarbon-contaminated aquifer and the significance for contaminant biodegradation,' *Water Resources Research*, **30**(5), 1561–1570.
- Vroblecky, D. A., Bradley, P. M., and Chapelle, F. H.: 1996, 'Influence of electron donor on the minimum sulfate concentration required for sulfate reduction in a petroleum hydrocarbon-contaminated aquifer,' *Environmental Science and Technology*, **30**, 1377–1381.
- Zhang, C., Grossman, E. L., and Ammerman, J. W.: 1998, 'Factors influencing methane distribution in Texas ground water,' *Ground Water*, **36**(1), 58–66.

Table E-1.1. LUFT site overview.

LUFT site location	Nature of release (commencement of site operations)	Hydrogeologic setting	Sampling event for data used in this study	Number of plume interior wells, background wells	Analytes
Castle Air Force Base (CAFB)	Aviation fuel (JP-4) leaking from above-ground and underground storage tanks, pipelines, and transfer lines (1940s)	Broad alluvial plain; mean depth-to-groundwater ~ 20 m	April, 1997	10, 9	TPH, BTEX, HCO ₃ ⁻ (as alkalinity), CH ₄ , E _h , Fe ²⁺ , Mn ²⁺ , O ₂ , NO ₃ ⁻ , pH, SO ₄ ²⁻
George Air Force Base (GAFB)	Aviation fuel (JP-4) leaking from fueling pits and associated piping (mid-1950s)	High desert alluvial fan; mean depth to groundwater ~ 40 m	March, 1992 – August, 1995 (mean values)	(8) ¹ , (8)	TPH, BTEX, HCO ₃ ⁻ (as alkalinity), CH ₄ , E _h , Fe ²⁺ , Mn ²⁺ , O ₂ , NO ₃ ⁻ , pH, SO ₄ ²⁻
Camp Pendleton Marine Corps Base (PMCB)	Base gasoline service station; leaks from underground tanks and piping systems (late 1950s)	Coastal canyon alluvium and fill; mean depth-to-groundwater ~ 5 m	April, 1997	8, 7	TPH, BTEX, HCO ₃ ⁻ (as alkalinity), CH ₄ , E _h , Fe ²⁺ , O ₂ , NO ₃ ⁻ , SO ₄ ²⁻
Presidio of San Francisco (PSF)	Gasoline and diesel released from above-ground storage tanks and piping systems (late 1930s)	Shallow marine deposits, organic-rich; mean depth-to-water ~ 1.5 m	April, 1997	7, 6	TPH, BTEX, HCO ₃ ⁻ (as alkalinity), CH ₄ , E _h , Fe ²⁺ , Mn ²⁺ , O ₂ , NO ₃ ⁻ , pH, SO ₄ ²⁻
Travis Air Force Base (TAFB)	Base gasoline service station; leaks from underground tanks and piping systems (late 1960s)	Broad alluvial plain; mean depth-to-groundwater ~ 4 m	August-September, 1995	13, 16	TPH, BTEX, HCO ₃ ⁻ (as alkalinity), CH ₄ , E _h , Fe ²⁺ , Mn ²⁺ , O ₂ , NO ₃ ⁻ , pH, SO ₄ ²⁻
Vandenberg Air Force Base (VAFB)	Base gasoline service station; leaks from underground tanks and piping systems (late 1960s)	Shallow marine deposits; mean depth-to-groundwater ~ 3 m	September, 1996	5, 9	TPH, BTEX, HCO ₃ ⁻ (as alkalinity), CH ₄ , E _h , Fe ²⁺ , Mn ²⁺ , NO ₃ ⁻ , pH, SO ₄ ²⁻

¹ Data from background wells with TPH concentrations below the applicable detection limit were not available from the George AFB LUFT site. Therefore, for comparative purposes, the median TPH concentration (approximately 0.1 ppm) was selected to delineate the plume interior well set from background.

Table E-1.2. Rank correlation coefficients between geochemical parameter values and TPH at the six LUFT sites.

Parameter	Expected correlation	CAFB	GAFB	PMCB	PSF	TAFB	VAFB
DO	-	-0.394	-0.382	-0.490	0.078	-0.326	N.A. ¹
NO ₃ ⁻	-	-0.648	-0.811	-0.181	-0.132	-0.562	-0.452
SO ₄ ²⁻	-	-0.760	-0.709	-0.403	0.202	-0.274	-0.694
pH	-	-0.176	-0.598	N.A.	-0.444	0.030	-0.387
E _h	-	-0.563	-0.891	-0.916	-0.334	-0.746	-0.830
Fe ²⁺	+	0.556	0.493	0.831	0.638	0.817	0.825
Mn ²⁺	+	0.559	0.737	N.A.	0.595	0.601	0.771
CH ₄	+	0.668	0.591	0.811	0.272	0.791	0.597
Alkalinity	+	0.571	0.497	0.718	0.445	0.549	0.190

¹ N.A. = not analyzed or not available.

Table E-1.3. Kruskal-Wallis confidence levels that geochemical parameter values differ significantly between plume interior and background samples.

Parameter	CAFB	GAFB	PMCB	PSF	TAFB	VAFB
DO	not signif.	not signif.	not signif.	not signif.	>90%	N.A. ¹
NO ₃ ⁻	95%	99%	not signif.	not signif.	99%	not signif.
SO ₄ ²⁻	99%	95%	not signif.	not signif.	not signif.	95%
pH	not signif.	95%	N.A.	90%	not signif.	not signif.
E _h	99%	99%	99%	not signif.	99%	99%
Fe ²⁺	95%	not signif.	90%	90%	99%	99%
Mn ²⁺	90%	90%	N.A.	90%	99%	99%
CH ₄	99%	not signif.	95%	90%	99%	90%
Alkalinity	95%	not signif.	95%	not signif.	99%	not signif.

¹ N.A. = not analyzed or not available.

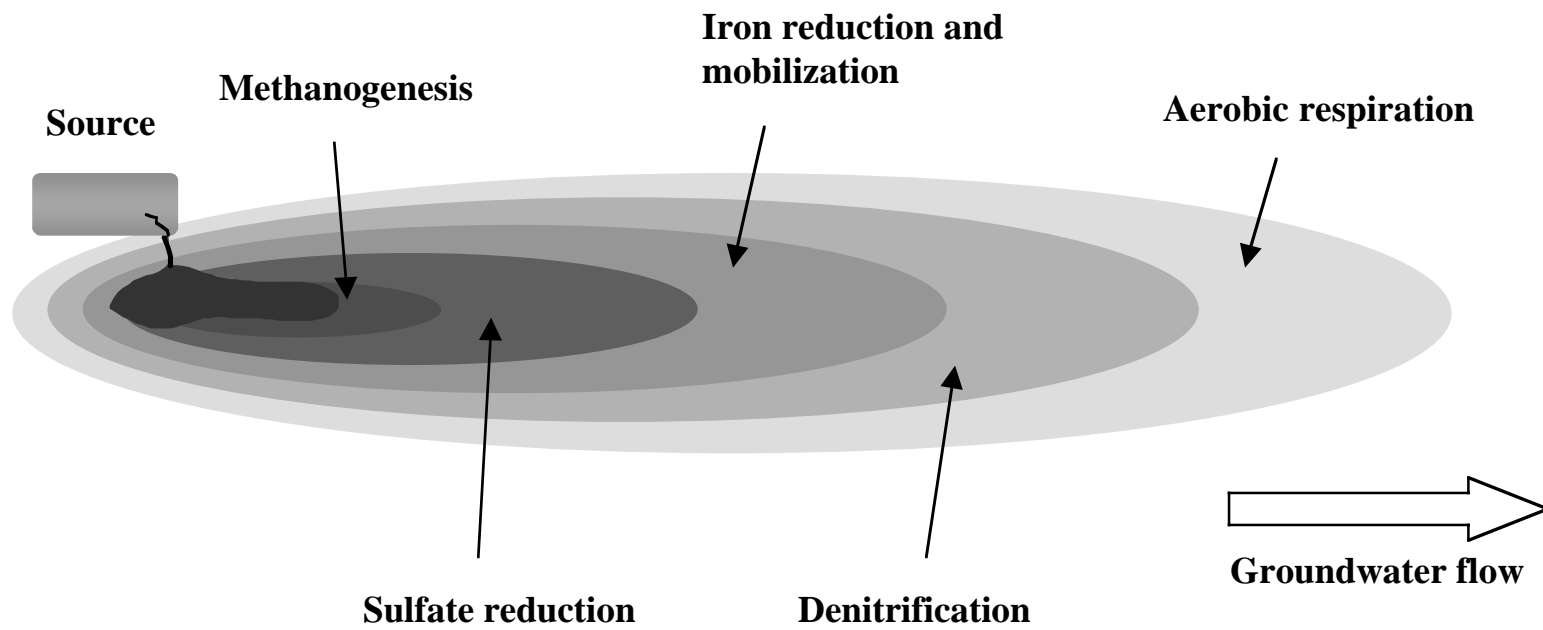


Figure E-1.1. A hypothetical fuel hydrocarbon release to groundwater with the associated impact on the local hydrogeochemistry.

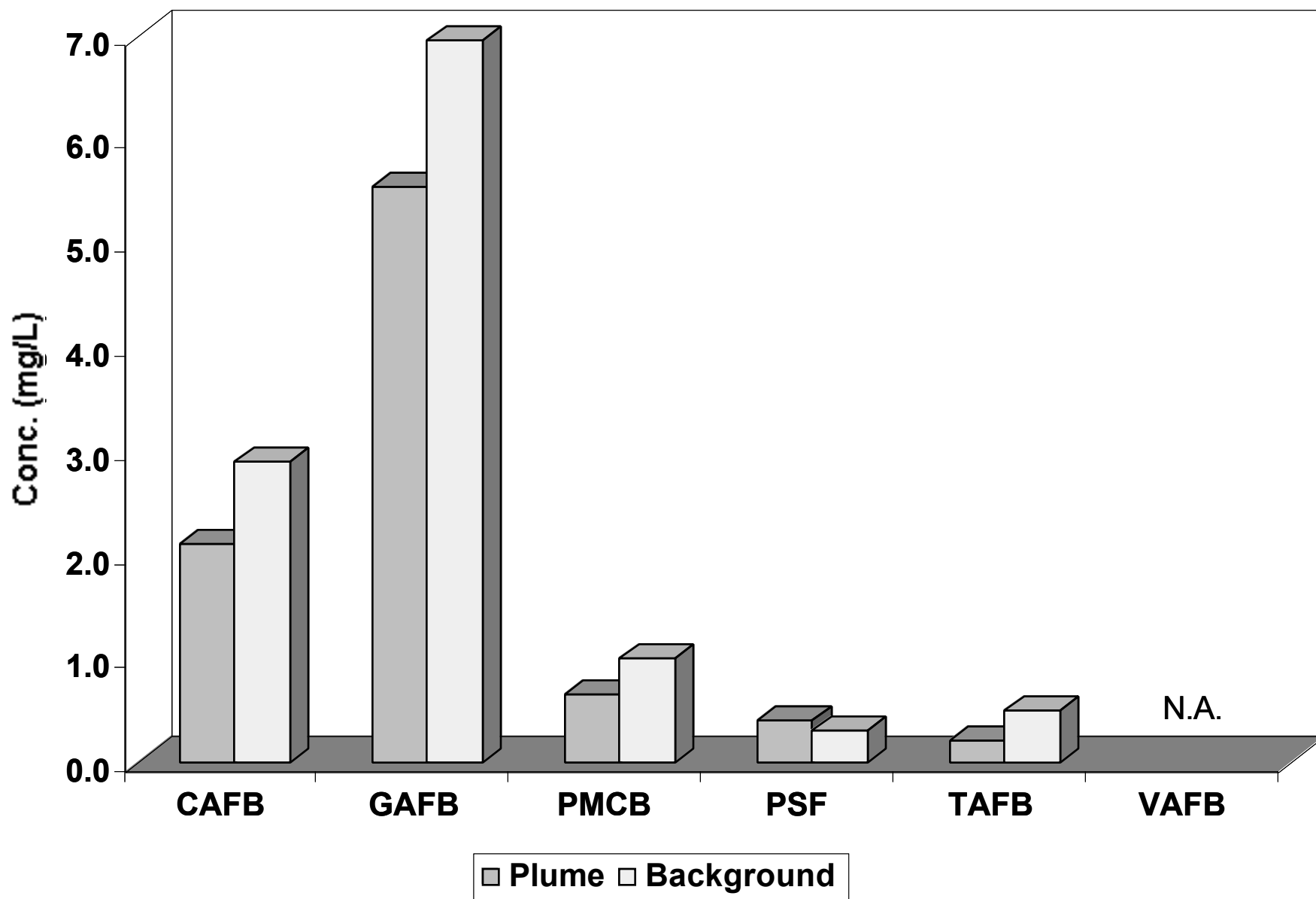


Figure E-1.2. Dissolved oxygen: comparison between median values from plume interior wells and median values from background wells.

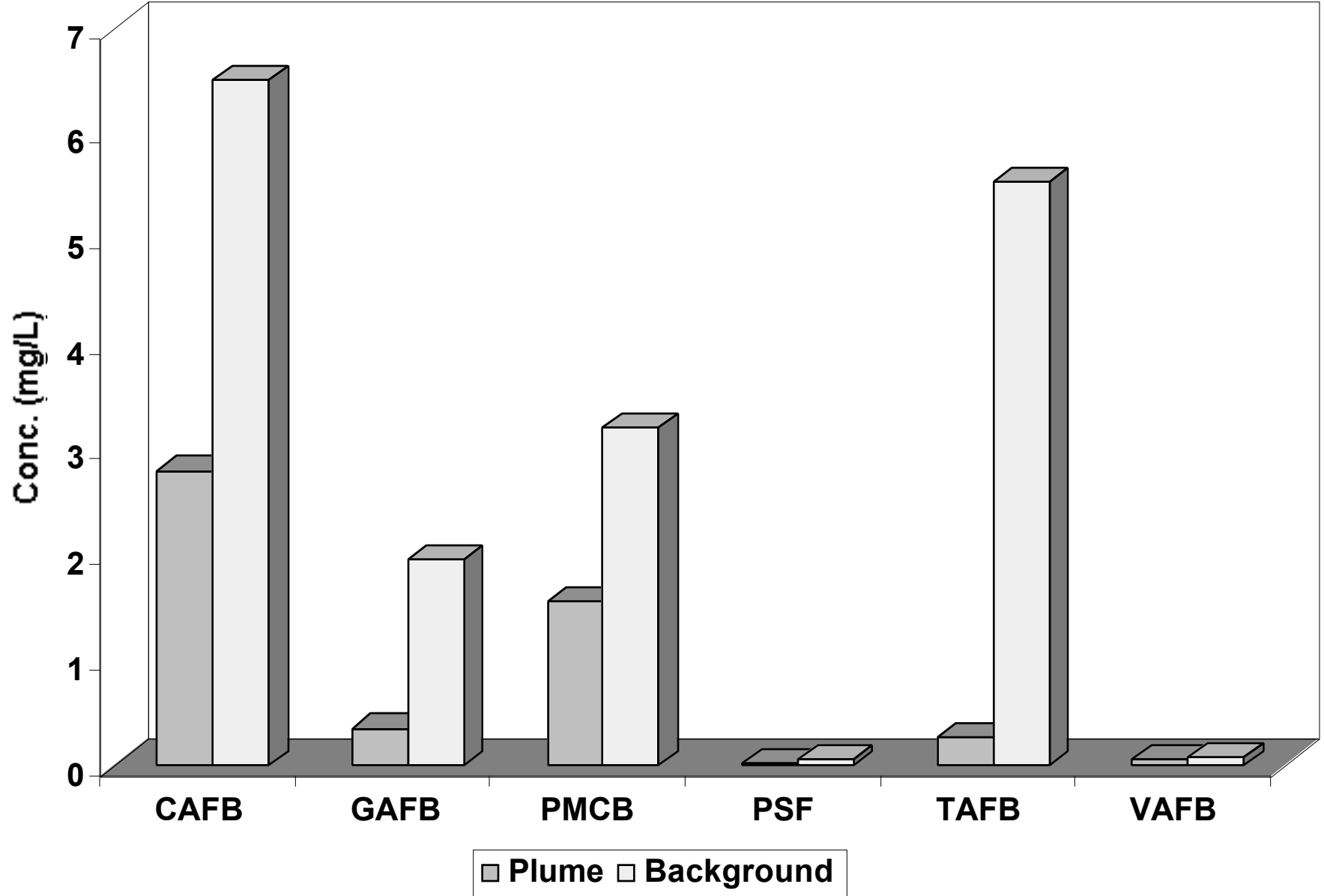


Figure E-1.3. Nitrate: comparison between median values form plume interior wells and median values form background wells.

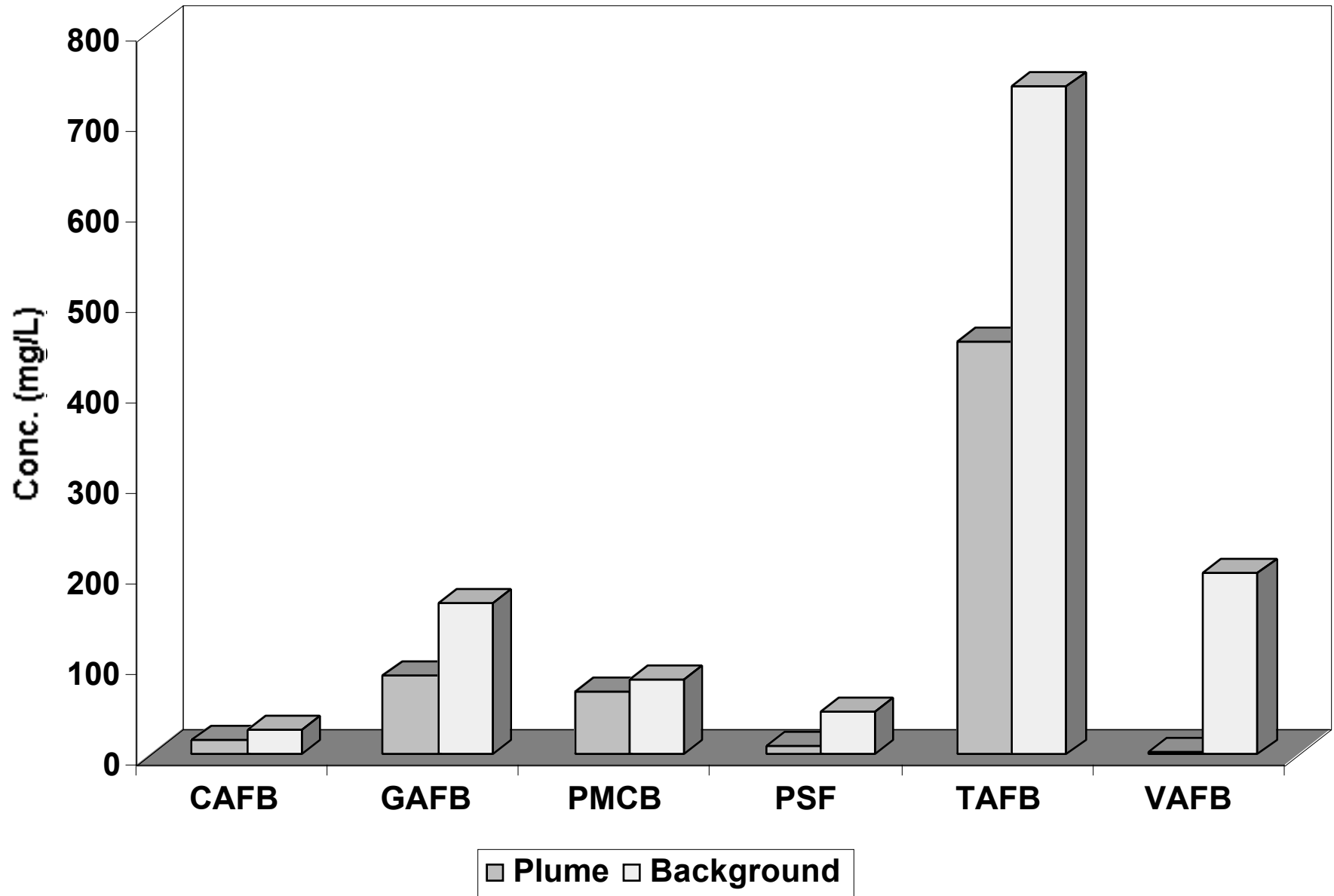


Figure E-1.4. Sulfate: comparison between median values from plume interior wells and median values from background wells.

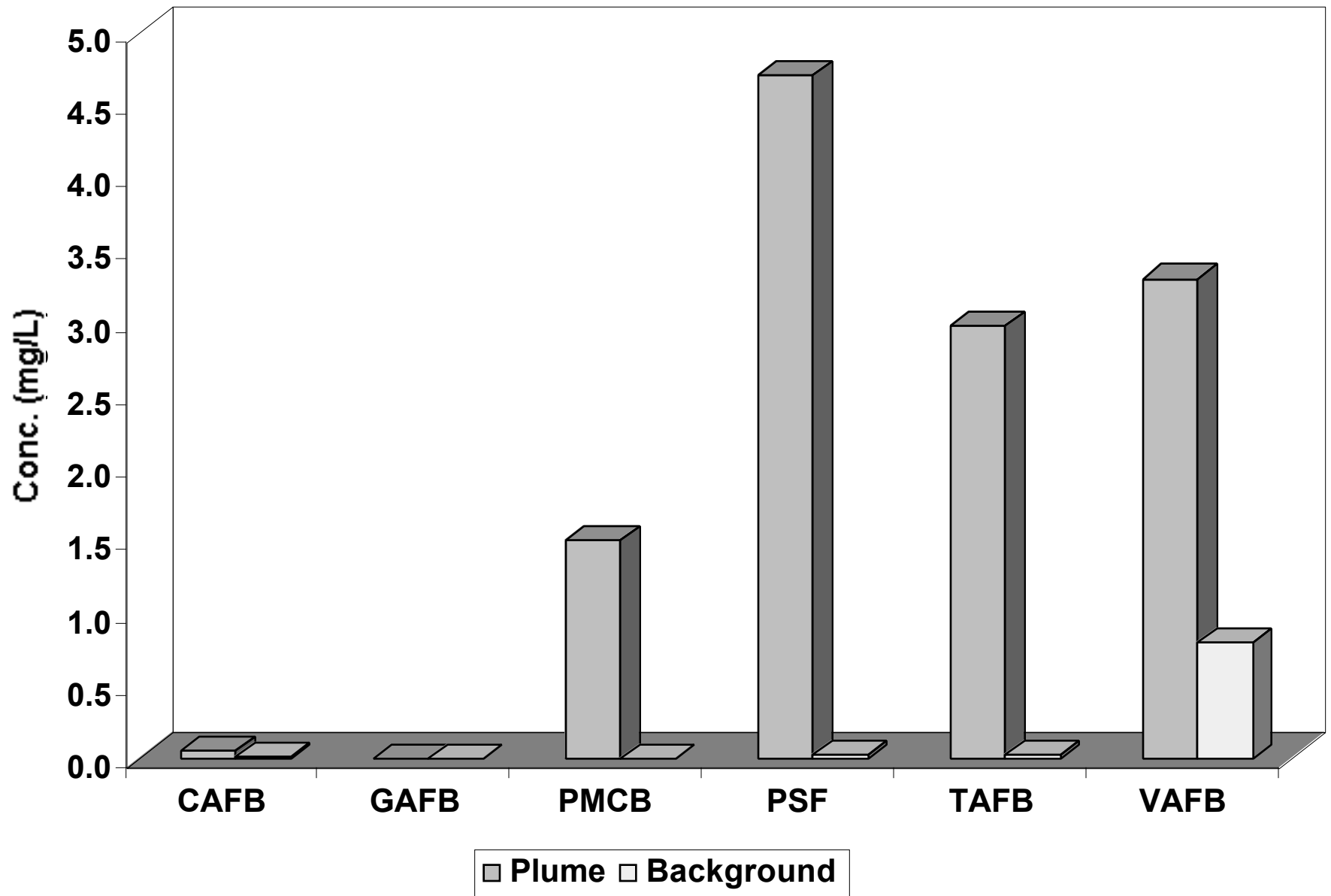


Figure E-1.5. Ferrous iron: comparison between median values from plume interior wells and median values from background wells.

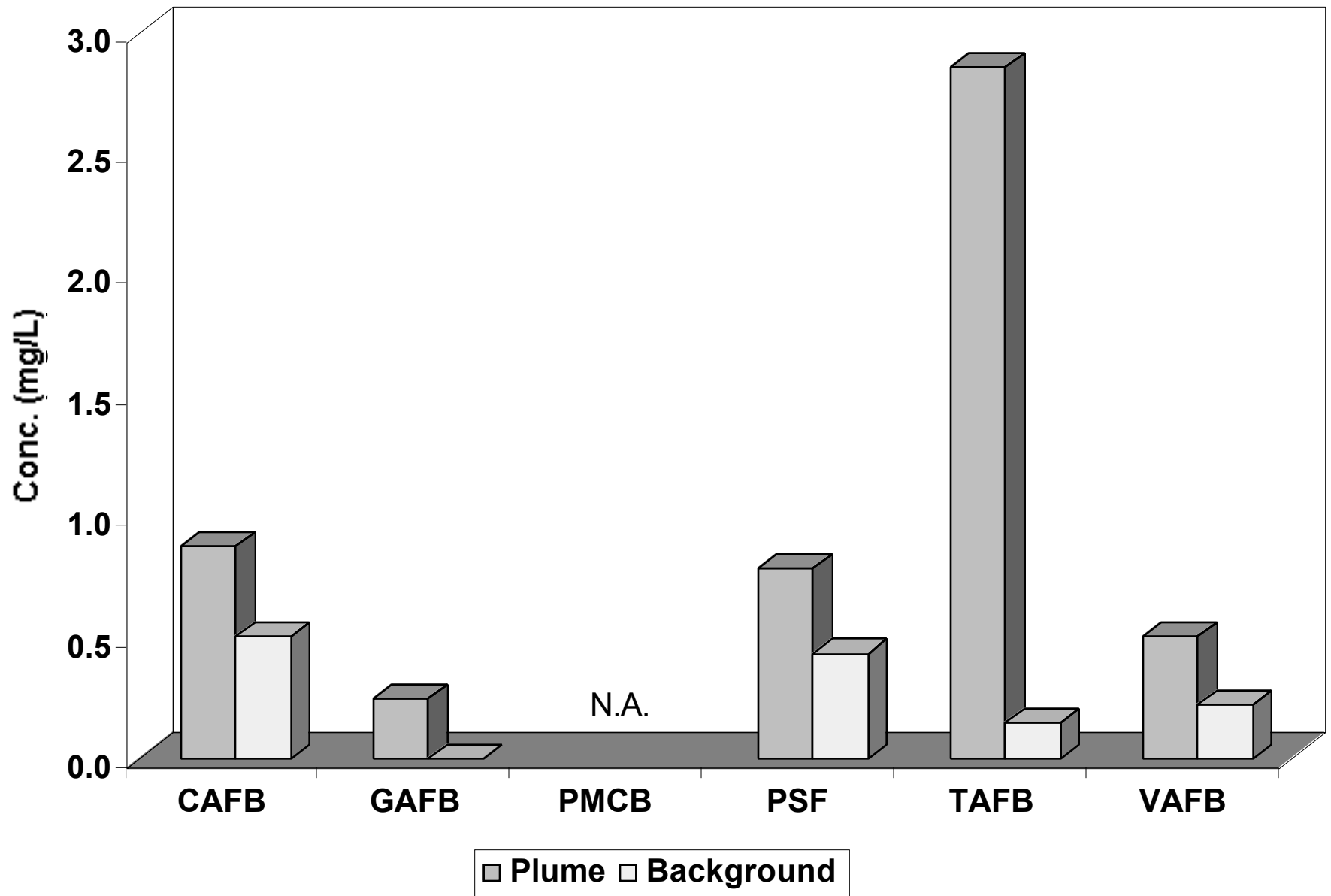


Figure E-1.6. Manganese: comparison between median values from plume interior wells and median values from background wells.

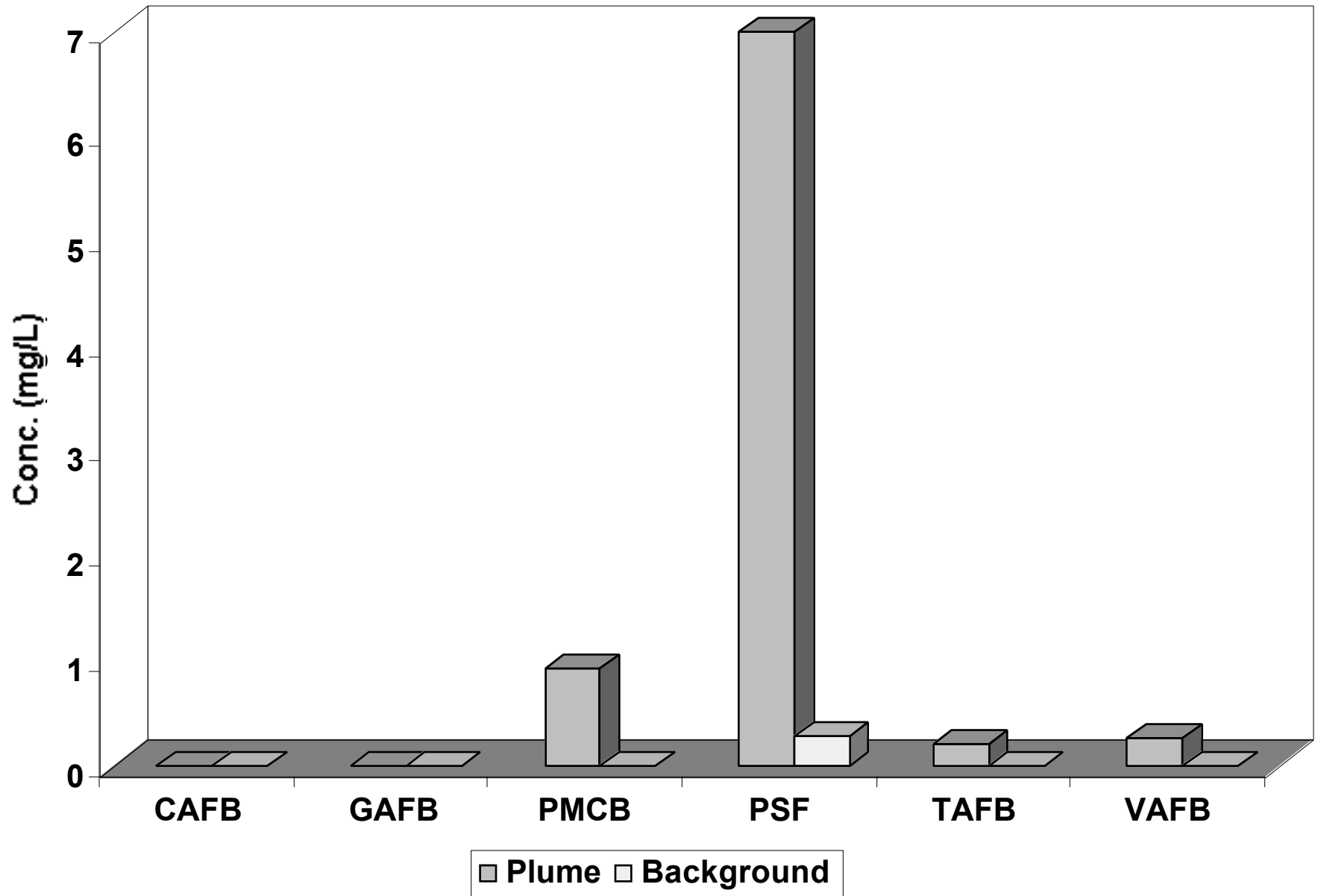


Figure E-1.7. Dissolved methane: comparison between median values from plume interior wells and median values from background wells.

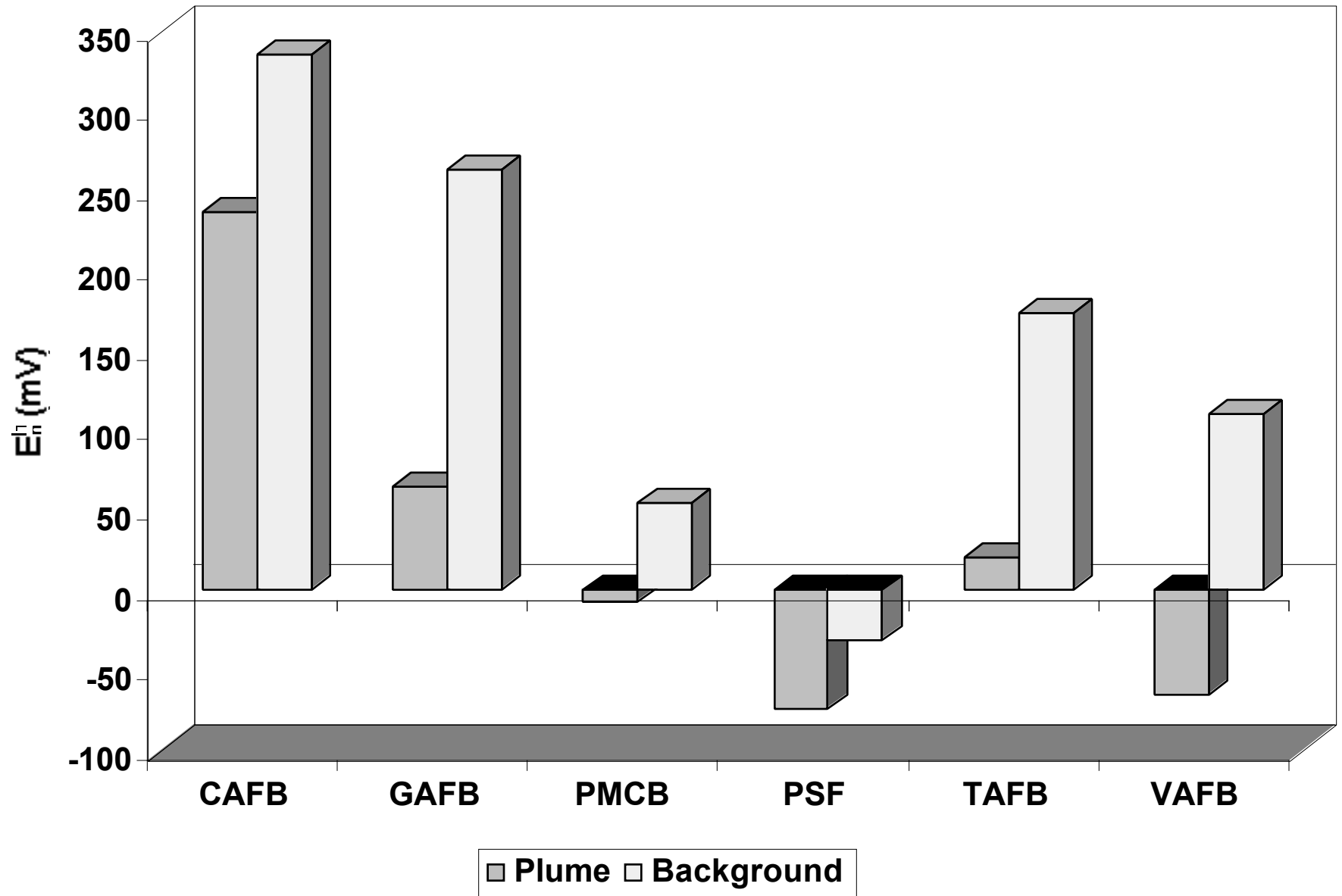


Figure E-1.8. E_h : comparison between median values from plume interior wells and median values from background wells.

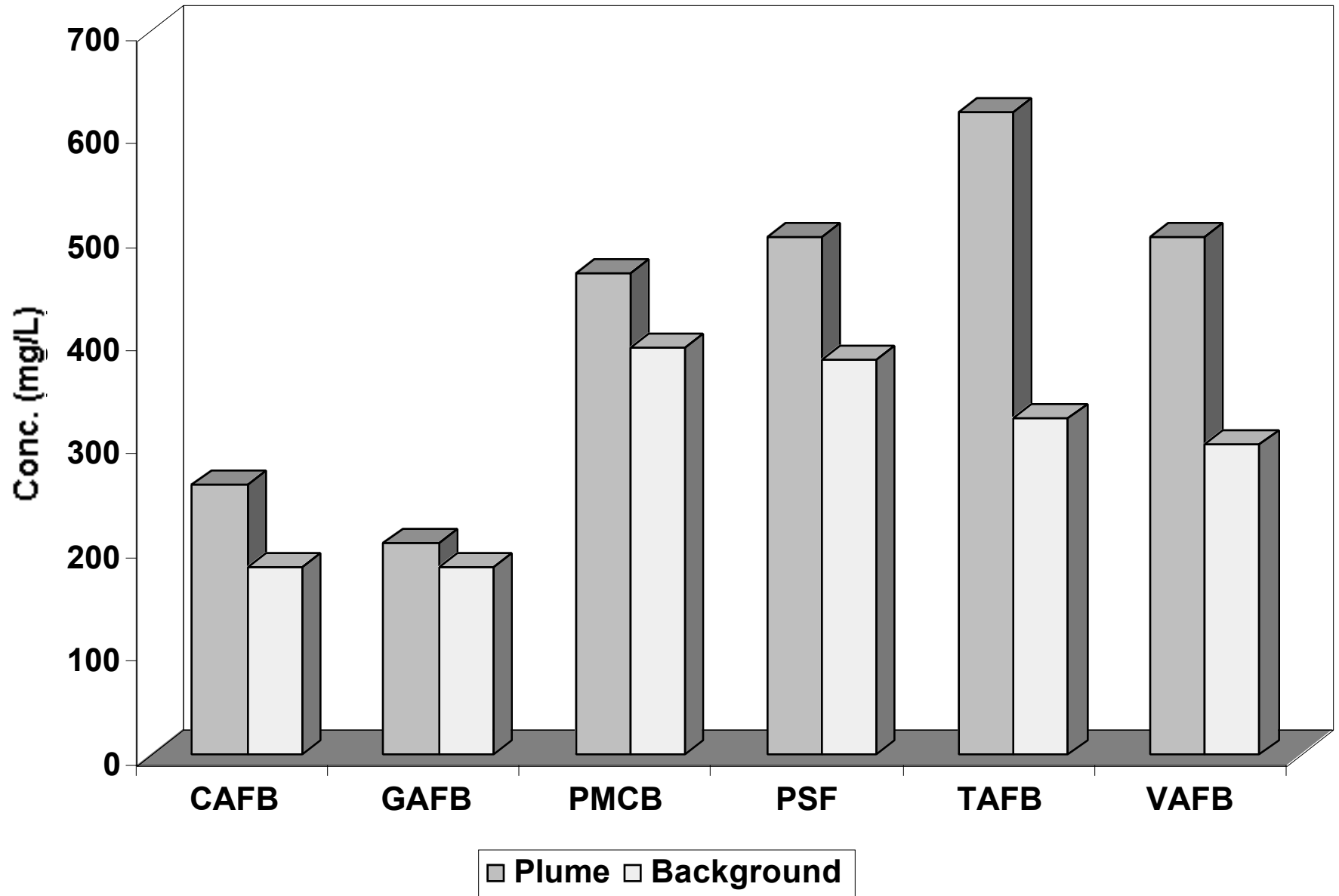


Figure E-1.9. Bicarbonate alkalinity: comparison between median values from plume interior wells and median values from background wells.

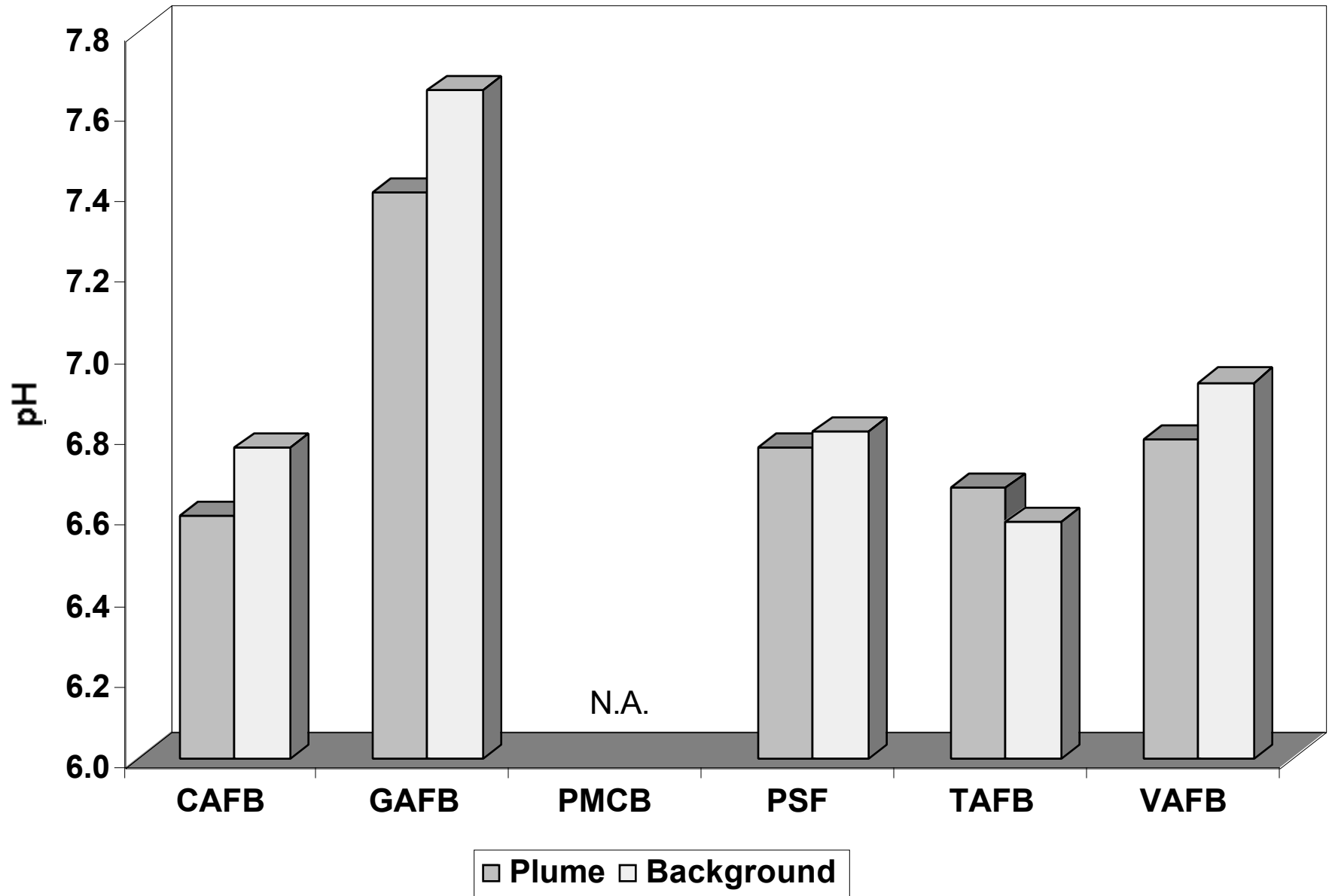


Figure E-1.10. pH: comparison between median values from plume interior wells and median values from background wells.

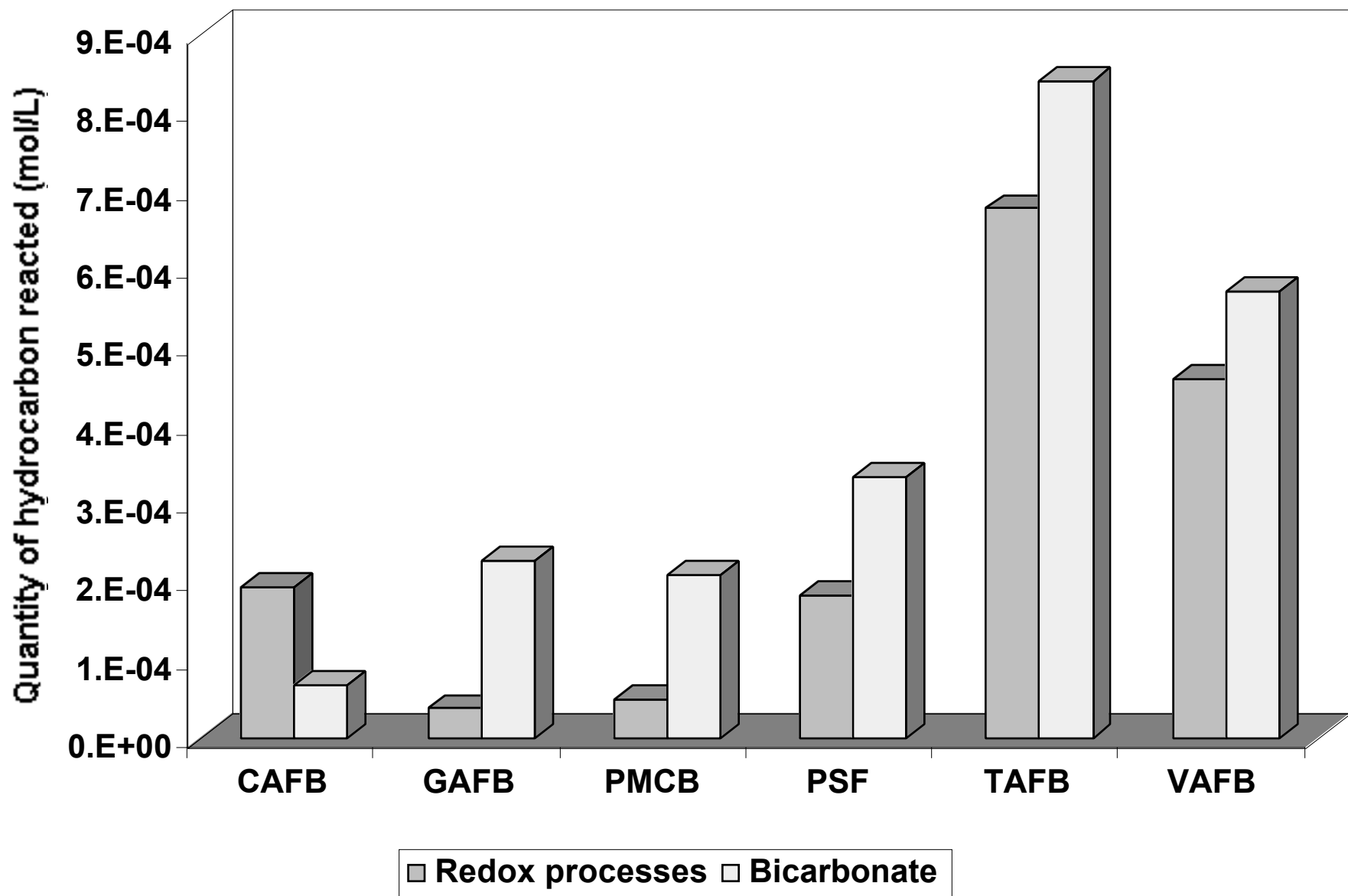


Figure E-1.11. Mass balance comparison of biotransformed fuel hydrocarbon mass implied by analysis of electron acceptor concentration differences and bicarbonate alkalinity.

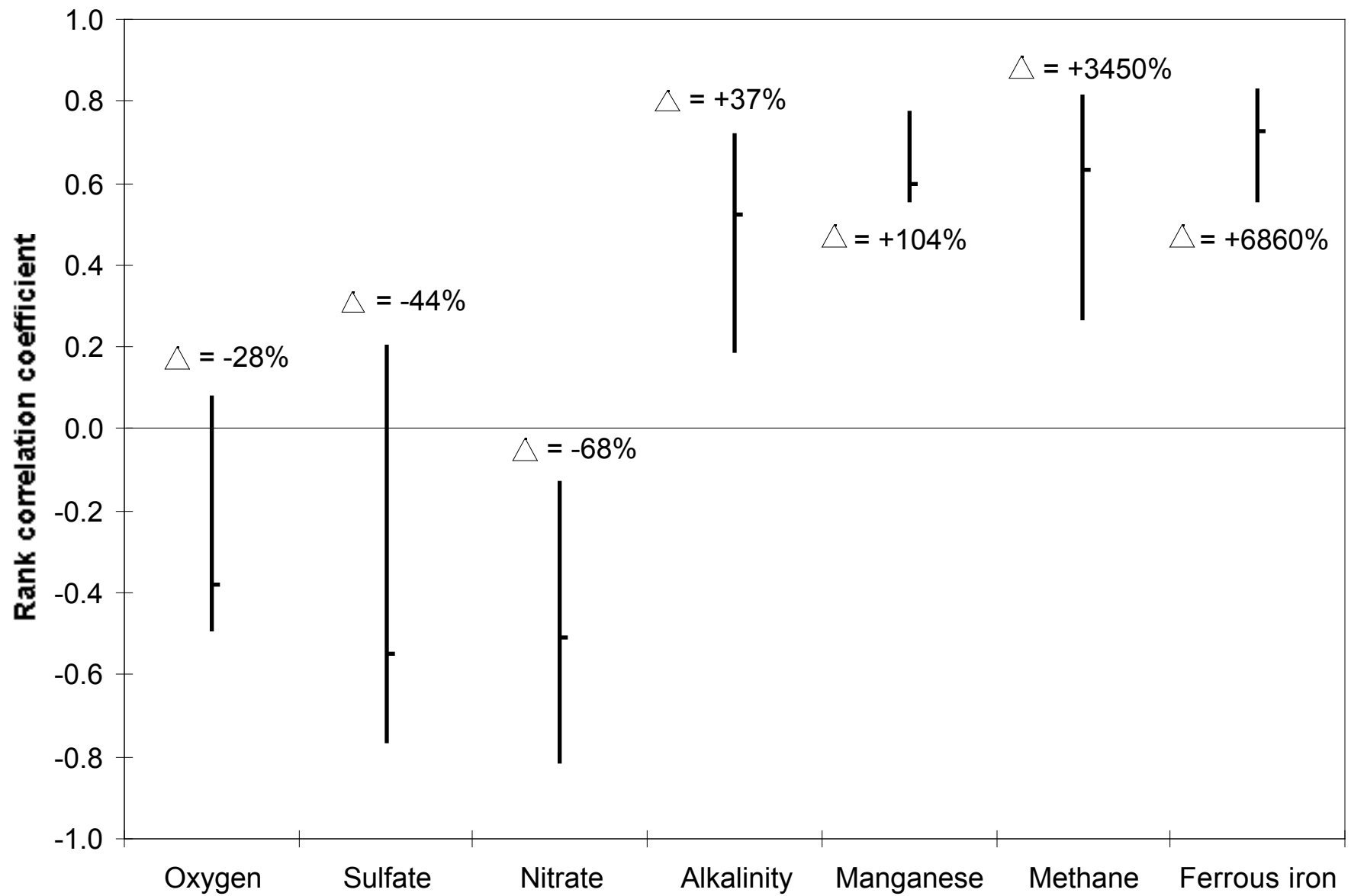


Figure E-1.12. Relationship between correlation coefficient (geochemical indicator value versus hydrocarbon concentration) and indicator signal-to-noise ratio.

Appendix E
Section E-2

**Uncertainty Analysis of Fuel Hydrocarbon
Biodegradation Signatures in Groundwater by
Probabilistic Modeling**

Appendix E (Section E-2)

Uncertainty Analyses of Fuel Hydrocarbon Biodegradation Signatures in Ground Water by Probabilistic Modeling

E-2.1. Introduction

Fuel hydrocarbon compounds (FHCs) associated with leaking underground fuel tanks (LUFTs) and pipelines are common ground water contaminants. Aromatic constituents such as benzene, toluene, ethylbenzene, and xylenes (BTEX) are of particular regulatory concern because of their relatively high solubility in water and possible long-term health effects (especially benzene). It is well-recognized that FHCs will biodegrade under a variety of conditions (e.g., Reinhard, Goodman, and Barker, 1984; Barker and others, 1986; Major et al., 1988; Grbic-Galic and Vogel, 1991; Haag et al., 1991; Kazumi et al., 1997). The recent study by Rice et al. (1995) showed that lengths of BTEX plumes in shallow ground water tend to be limited to distances less than approximately 80 meters from the source (based on California data). This finding was supported by Buscheck et al. (1996) as well as by Mace et al. (1997). Natural attenuation mechanisms (i.e., primarily biodegradation) were cited as a probable explanation for plume length limitation.

Regulators, site stakeholders, and the scientific community have begun to recognize that natural attenuation processes can effectively remediate ground water contaminated with FHCs. To assess the risk to potential downgradient receptors, transport models are often used to predict future plume behavior and cleanup time. However, even when employing simple models, uncertainty in ground water velocity, mean contaminant degradation rate, dispersivities, and the nature of the source term (i.e. location, release history, total contaminant mass) create cumulative uncertainties in projected plume behavior. Moreover, because models are calibrated to existing or historical contaminant concentration data, the effect of parameter uncertainty is to produce non-unique solutions to the contaminant transport problem. Thus, to improve practical decision-making processes associated with LUFT sites, uncertainty in model forecasts, and the relationship to parameter uncertainty, must be quantified and analyzed.

The problem of constraining parameter and forecast uncertainty often requires extensive data collection (e.g., installation of numerous monitoring wells) and thus additional costs. However, biodegrading FHCs often measurably affect the local inorganic geochemistry through coupled oxidation-reduction reactions which are mediated by microorganisms in the subsurface (e.g., Lovley et al., 1989; Cozzarelli and Baedeker, 1992; Baedeker et al., 1993; Vroblesky and Chapelle, 1994; Borden et al, 1995; Vroblesky et al., 1996). For example, electron acceptors such as oxygen, nitrate, or sulfate may be locally depleted in association with FHC oxidation, whereas chemically-reduced species (e.g., sulfide, methane) or mineralization products (i.e., carbon dioxide) may accumulate. Because these data are often collected as part of routine ground water sampling activities, they may be used to provide constraints on the relationships between mean

degradation rates, source mass, and other factors. The key to using these constraints to reduce uncertainty is to dynamically link geochemical indicator concentration data to the contaminant transport model.

To quantify forecast uncertainties, a probabilistic modeling approach has been developed which links the reactive transport of FHCs to the local geochemistry using superposition of an analytical transport model, reaction stoichiometry, and Monte Carlo simulation. This approach allows uncertainties in hydrogeologic data (e.g., hydraulic conductivity, hydraulic gradient magnitude and direction) and geochemical data (e.g., background electron acceptor concentrations, degradation rates) to be translated into uncertainties regarding forecast contaminant and electron acceptor concentrations at individual wells. Sensitivity analyses of these results can provide insights into the critical data needed for quantifying the behavior of plumes.

E-2.2. Modeling Approach

Wilson and Miller (1978) presented an analytical solution for solute transport in a homogeneous, infinite aquifer of constant thickness with a uniform fluid flow field assuming an instantaneous point source. Modified to account for retardation and a continuous source release, this solution may be written as,

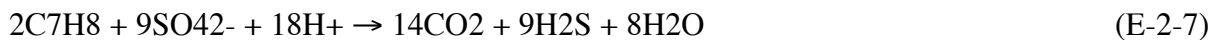
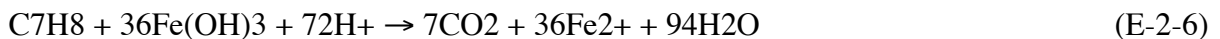
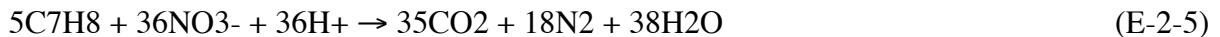
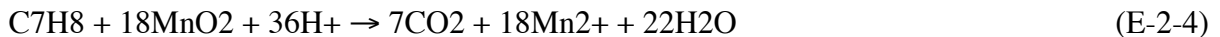
$$c(x, y, t) = \int_{\tau=0}^{\tau=t} \frac{dM}{4\pi\phi\tau H\sqrt{D_l D_t}} \exp \left[-\frac{(x - \frac{v}{R}\tau)^2}{4\frac{D_l}{R}\tau} - \frac{y^2}{4\frac{D_t}{R}\tau} - \lambda\tau \right] d\tau \quad (\text{E-2-1})$$

where dM is the mass introduced into the system per unit time, ϕ the porosity, H the aquifer thickness, D_l and D_t the longitudinal and transverse dispersion coefficients, respectively; v the ground water velocity, R the retardation coefficient, λ the first-order decay coefficient, x and y , the distances between the source location and the monitor point in the longitudinal and transverse directions, respectively, and t the elapsed time between source introduction and sampling time. Although Eq. (E-2-1) is a highly idealized conceptualization of solute transport, it does serve as a reasonable probability distribution model of contaminant concentrations in space and time. The uniform first-order kinetic model is a simplifying assumption which neglects the influences of microbial growth on substrate utilization rates. Moreover, it does not account for variability in degradation rates associated with different biogeochemical redox regimes. Nevertheless, as a screening model for engineering decision-making with sparse field data, the first-order kinetic model often serves as a useful first approximation (MacIntyre et al., 1993; Wilson et al., 1995; Buscheck et al., 1996), particularly when redox conditions are largely anaerobic (Rafai et al., 1987).

At a given location (x, y) , the cumulative FHC quantity which has undergone biodegradation, ΔC , is given by superposition according to,

$$\Delta c(x, y, t) = \int_{\tau=0}^{\tau=t} \frac{dM}{4\pi\phi\tau H\sqrt{D_1 D_t}} \exp \left[-\frac{(x - \frac{v}{R}\tau)^2}{4\frac{D_1}{R}\tau} - \frac{y^2}{4\frac{D_t}{R}\tau} \right] d\tau - \int_{\tau=0}^{\tau=t} \frac{dM}{4\pi\phi\tau H\sqrt{D_1 D_t}} \exp \left[-\frac{(x - \frac{v}{R}\tau)^2}{4\frac{D_1}{R}\tau} - \frac{y^2}{4\frac{D_t}{R}\tau} - \lambda\tau \right] d\tau \quad (\text{E-2-2})$$

Eq. (E-2-2) describes the amount of FHC which has been previously transformed upgradient. Using toluene, C₇H₈, as a surrogate for the cumulative concentration of FHCs, the oxidation of Δc must be balanced stoichiometrically by the reduction of one or more electron acceptors as given by,



These reactions are listed by decreasing thermodynamic favorability, a sequence generally followed by microorganisms to obtain the maximum energy benefit. To address this sequence in the model, the quantity of FHC biodegraded at a given point is first calculated by Eq. (E-2-2). Electron acceptor concentrations are then adjusted, in sequence, based Eqs. (E-2-3) through (E-2-8) until all of the mineralized FHC is accounted for in the mass balance. For iron and manganese, the electron acceptor species consist of solid-phase mineral oxides. For modeling purposes, these may be represented as fictitious aqueous species based upon observed concentrations of Fe²⁺ and Mn²⁺ within the hydrocarbon plume. Methane concentrations may be predicted directly using Eq. (E-2-8). Assuming that most of the carbon dioxide produced in the FHC mineralization reactions is converted to bicarbonate under near-neutral pH conditions, local changes in carbon dioxide (bicarbonate) can be estimated by Eqs. (E-2-3) through (E-2-8). At present, the model ignores the conversion of a fraction of the hydrocarbon material into cell biomass.

In cases of significant retardation of FHCs resulting from adsorption, the model is not applicable. This is because the superposition of the analytical model assumes that all constituents are characterized by the same mobility. Thus, any scenarios which assume a retardation coefficient greater than 1.0 for FHCs assume the same retardation for all electron acceptors, methane, and bicarbonate. This may lead to significant error in certain instances.

Probabilistic modeling of dynamic transport involves utilizing user-specified probability distributions of physical and chemical model parameters, representing uncertainty in data, to produce forecasts through multiple Monte Carlo realizations. Monte Carlo analyses are routinely used in engineering probability forecasting applications (Ang and Tang, 1984, Press et al., 1992). Woodbury et al. (1995) discuss the use of Monte Carlo analyses in practical ground water engineering applications. Each Monte Carlo simulation in this study consisted of executing 1,000 realizations within the prescribed parameter space at each monitoring well location and tallying the forecast concentrations. Forecast probabilities were then compared to measured concentrations of each constituent.

All calculations in this study were conducted using commercial spreadsheet software (Decisioneering, Inc., 1996). Eq. (E-2-2) was integrated numerically using the midpoint rule.

E-2.3. Example Application

The model developed in this study was applied to ground water quality data collected from the North-South Gas Station (NSGS) site at Travis Air Force Base in Fairfield, California. The site consists of two gasoline service stations from which unknown quantities of gasoline were released into the subsurface from LUFTs between the 1960s and the late 1980s. Site geology is characterized by unconsolidated Holocene and Pleistocene alluvial clays, silts, sands, and gravels. Ground water is encountered at a depth of approximately 4 to 5 meters below surface under semi-confined conditions. The ground water flow direction is to the south-southeast at a rate of approximately 10-15 m/yr. Monitoring well data indicate a dissolved BTEX plume extending some 100 meters downgradient of the South Gas Station (Parsons Engineering Science, 1996). Differences in geochemical indicator parameter values between BTEX-contaminated and uncontaminated wells are shown on Table E-2.1. Differences in indicator concentrations between plume interior and background strongly suggest that sulfate reduction is the most important biodegradation mechanism at the site, accounting for over 95% of the inferred electron acceptor utilization.

The BTEX plume at the NSGS site, based on August-September, 1995 monitoring well data, is shown on Fig. E-2.1. Two modeled hydrocarbon plume realizations, using the example parameter values listed on Table E-2.2 (based largely on site data), are also shown on the figure. For modeling purposes, BTEX is assumed to represent all of the biodegradable portion of the FHCs; toluene is in turn used as a surrogate for BTEX. Despite the differences in key parameters between the two realizations, both modeled plumes qualitatively resemble the observed distribution. Measured and modeled sulfate and bicarbonate concentration distributions are shown on Figs. E-2.2 and E-2.3, respectively. Again, a general qualitative correlation exists between the field data and the simulated distributions for both realizations. Similar qualitative correlations also exist with respect to the other geochemical indicators (data not shown).

Clearly, within a parameter space constrained by reasonable expectations for hydrogeologic and geochemical variables, a number of potential solutions exist which may reproduce general trends in field observations. Ideally, one approach for reconciling parameter estimates to achieve the best match to all observed data is through non-linear optimization, using Newton-Raphson iteration or some other error-minimization technique. However, such an approach fails to adequately address uncertainties and thus provides no means for quantifying confidence in the results. An alternative approach is to utilize multiple realizations, with parameters chosen from within prescribed probability distributions, to produce ranges of forecast values. Sensitivity of results to model parameters may then be assessed.

For the NSGS site model, transport model parameter assumptions are listed on Table E-2.3, along with background distributions of sulfate and bicarbonate. Background probability distributions for the remaining geochemical indicators (not shown) were also based on fitting monitoring data. These probability distributions reflect limited empirical observations or postulations and do not necessarily represent the true parameter distribution functions, which are unknown. For example, mean hydraulic conductivity probability distributions reflect estimated hydraulic conductivities from a small number of pumping tests and slug tests. As such, only a limited portion of the true distribution of sediment types present in the subsurface is represented, so forecast results must always be treated with the appropriate degree of caution.

Forecast median and measured concentrations of total BTEX, sulfate (the dominant electron acceptor), and bicarbonate (the most widespread indicator of mineralization) are shown on Figs. E-2.4 through E-2.6, respectively. Error bars indicate the forecast confidence intervals delineated by the 25th and 75th percentiles. Measured BTEX concentrations (Fig. E-2.4) in 9 out of 14 wells with detectable BTEX concentrations fall between the 25th and 75th forecast percentiles. Median forecast concentrations exceed measured concentrations to varying degrees in 6 of the 14 wells. Correlation between median forecast values and field data is marginal, with a rank-based correlation coefficient of only 0.51. Forecast BTEX concentrations are also characterized by very high uncertainties. With regard to sulfate (Fig. E-2.5), aside from three outlier wells characterized by very high sulfate concentrations, measured values generally fall within the middle two quartiles (18 out of 25 wells). Median forecast values exceed field data in 16 of 25 wells. Again, the degree of correlation is marginal ($R = 0.40$ by rank correlation) and a high degree of uncertainty exists in the forecasts. Forecast bicarbonate concentrations (Fig. E-2.6) reflect moderate agreement with observations, with measured values falling within the middle two quartiles in 15 out of 28 wells. Median forecast values exceed field data in 15 of 28 wells. The rank-based correlation coefficient between median forecast values and field data is 0.56. Forecasts of other geochemical indicators (dissolved oxygen, nitrate, iron, manganese, methane) are not shown because of the large number of non-detections, either in observation data or in forecast values.

For each of the three parameters, the number of forecast median values which exceed measured concentrations is roughly equal to half of the number of observations, indicating a lack of a strong systematic bias in forecast values. This suggests that the essential parameter ranges chosen do not reflect gross overestimates or underestimates of such factors as source mass or degradation rate. The partial degree of correlation between forecast values and field data also suggests that the model is reflecting the coupled transport and biogeochemical processes occurring at the site to some degree. However, the main feature apparent in the simulation results is the high degree of uncertainty associated with forecast concentrations at any one monitoring location, even within the fairly well-constrained parameter space outlined on Table E-2.3. Thus, the question of which

parameters exert the most significant influence on various forecasts emerges as the central issue of this study.

E-2.4. Sensitivity Analyses

Sensitivity analyses provide insight into the impact of parameter probability distributions on uncertainty in forecast variability. To quantify sensitivity, parameters and forecasts are rank-correlated. Rank correlation offers an advantage over normal (value) correlation in that it can address strongly nonlinear trends in the data and can suppress the effects of outliers in skewing the correlation coefficient (Isaaks and Srivastava, 1989). Rank correlation involves assigning ranks to both the dependent variable (the forecast) and the independent variable (the parameter) and performing a linear regression on the corresponding rank sets. The resulting correlation coefficients are then tallied for each forecast and normalized. This yields the relative contribution to variance of each parameter (e.g., hydraulic conductivity, source location, background concentration) to each forecast (concentrations of total BTEX and geochemical indicators at each well).

Parameter sensitivities for forecast BTEX concentrations as a function of distance from the source area are shown on Fig. E-2.7. A variety of factors appear to impact forecast variability in the source area, particularly uncertainty in the degradation rate, source location (southern gas station), and hydraulic conductivity. Further downgradient, uncertainty in the ground water velocity, as indicated by uncertainties in conductivity and gradient, is more important, while factors pertaining to the nature of the source term(s) are less significant. In particular, uncertainty in the degradation rate, perhaps the most significant factor impacting forecasts in the source area, becomes less significant by comparison further downgradient. It must be emphasized that at other sites with different parameter distributions, the contributions to uncertainty will differ from the results observed with respect to this example site.

Parameter sensitivities for selected geochemical indicators in MW-138 and MP-7 (monitor wells in the source vicinity and far downgradient at the NSGS site, respectively) are shown on Table E-2.4. The pattern of parameter sensitivity appears to be more complex in comparison to that of BTEX. For sulfate, uncertainty in the background concentration dominates forecast variance, both near the source area and far downgradient (apparent sensitivity to background bicarbonate results from the prescribed correlation between the two parameters). This reflects the high variability and high concentrations of background sulfate values. In contrast, uncertainties in bicarbonate concentrations primarily reflect uncertainties in other factors (ground water velocity parameters, source location) near the source area in addition to uncertainty in background concentration. This is an indication of the strong influence of FHC mineralization on bicarbonate concentrations near the source area. Further downgradient, uncertainty in the background concentration dominates. Forecast methane levels in the source area are significantly affected by uncertainties in the background sulfate concentration. This is a result of the sequential electron acceptor reaction sequence assumed by the model: Sulfate must be fully exhausted before methanogenesis is assumed to occur. Uncertainty in forecast oxygen levels far downgradient of the plume is dominated by uncertainty in the ground water velocity. Similar patterns are associated with nitrate, iron, and manganese concentrations (not shown). Because of the relatively low concentrations involved, each of these electron acceptors is likely to be entirely utilized in the

source area. Thus, changes in concentration in the downgradient direction are in large part a reflection of the migration rate of the anaerobic shadow emerging from the BTEX plume.

Surprisingly, variances in forecast geochemical indicator concentrations do not appear to be sensitive, in a relative sense, to uncertainty in the BTEX degradation rate. In the source area, this is because uncertainty in the background concentrations dominates the forecast concentrations. Downgradient, forecast concentrations are most affected by uncertainty in the ground water velocity, which determines the extent of the geochemical signature migration. Again, it should be noted that at other sites with different parameter distributions, the contributions to uncertainty will differ. This may be especially true with regard to sulfate and bicarbonate, which are characterized by very high background values at the NSGS site.

E-2.5. General Applicability of the Approach

Aside from the specified variability in model parameters, a number of other factors may contribute to the discrepancies between forecast concentrations and field data. These include physical heterogeneities in the flow field not adequately addressed by the dispersion model, transport in the third dimension (including dilution effects associated with long well screens), complex source release history, significant retardation effects, and spatially-variable biodegradation rates. Another potential source of error for the example application is the use of BTEX concentrations (represented by toluene as a surrogate) as a mass balance constraint on geochemical indicator concentrations. In reality, non-BTEX components present in the gasoline mixture will also biodegrade and influence the local geochemistry as well. Nevertheless, given the large uncertainties associated with BTEX concentrations in the existing model (Fig. E-2.4), this effect may be relatively small by comparison at the NSGS site.

Despite these potential shortcomings, this approach presents a reasonable probability distribution model for fuel hydrocarbon and geochemical indicator concentrations in the absence of a more detailed conceptual model. As such, this approach should be applicable to a variety of LUFT sites which have been characterized to a similar degree. Nevertheless, the findings pertaining to the BTEX plume analyses at the NSGS site are site-specific, reflecting a particular hydrogeologic and biogeochemical setting, and may or may not be characteristic of other LUFT cases. This pertains not only to the ranges of forecast concentrations but to parameter sensitivities as well.

The value in applying this technique to LUFT sites is that the uncertainties associated with predictive modeling may be quantified. Biodegradation tends to limit the migration of FHC plumes; the input of dissolved FHCs from residual sources is balanced by losses through biodegradation, integrated over the extent of the plume. Hence, biodegradation can protect downgradient receptors by preventing migration of the plume beyond a certain distance from the source. Variances in concentration forecasts thus translate into uncertainties in receptor impact. This information allows for more informed cleanup decision-making from a regulatory perspective. If uncertainties must be reduced in specific cases, further data collection may be recommended and more detailed modeling attempted. In this way, the extent to which a site must be characterized to develop appropriate engineering solutions may be determined in an objective and systematic manner.

E-2.6. References

- Ang, A. H-S., W. H. Tang (1984), "Probability Concepts in Engineering Planning and Design, v. 2: Decision, Risk, and Reliability" (John Wiley & Sons, New York).
- Baedecker, M. J., I. M. Cozzarelli, R. P. Eganhouse, D. I. Siegel, and P. C. Bennett (1993), "Crude oil in a shallow sand and gravel aquifer, 3. Biogeochemical reactions and mass balance modeling in anoxic ground water," *Applied Geochemistry* **8**(6), pp. 569–586.
- Barker, J. F., J. S. Tessman, P. E. Plotz, and M. Reinhard (1986), "The organic geochemistry of a sanitary landfill leachate plume," *Journal of Contaminant Hydrology* **1**(1/2), 171–189.
- Borden, R. C., C. A. Gomez, and M. T. Becker (1995), "Geochemical indicators of intrinsic bioremediation," *Ground Water* **33**(2), 180–189.
- Buscheck, T. E., D. C. Wickland, and D. L. Kuehne (1996), "Multiple lines of evidence to demonstrate natural attenuation of petroleum hydrocarbons," in *Proceedings from the Conference on Petroleum Hydrocarbons and Organic Chemicals in Ground Water*, National Ground water Association/API, Houston, Texas, November 13–15.
- Chapelle, F. H., P. M. Bradley, D. R. Lovley, and D. A. Vroblesky (1996), "Measuring rates of biodegradation in a contaminated aquifer using field and laboratory methods," *Ground Water* **34**(4), 691–698.
- Cozzarelli, I. M., and M. J. Baedecker (1992), "Oxidation of hydrocarbons coupled to reduction of inorganic species in ground water," in *Water-Rock Interactions*, Y. K. Kharaka, and A. S. Maest, and A. A. Balkema, Eds. (Rotterdam, Netherlands), pp. 275–278.
- Decisioneering, Inc. (1996), "Crystal Ball: Forecasting and Risk Analysis for Spreadsheet Users," Decisioneering, Inc., Aurora, Colorado.
- Grbic-Galic, D., and T. M. Vogel. (1987), "Transformation of toluene and benzene by mixed methanogenic cultures," *Applied and Environmental Microbiology* **53**(2), 254–260.
- Haag, F., M. Reinhard, and P. L. McCarty (1991), "Degradation of toluene and p-xylene" in *Anaerobic microcosms: Evidence for sulfate as a terminal electron acceptor*, *Environmental Toxicology and Chemistry* **10**(11), 1379–1390.
- Isaaks, E. H., and R. M. Srivastava (1989), "An Introduction to Applied Geostatistics" (Oxford University Press, Oxford, England).
- Kazumi, J., M. E. Caldwell, J. M. Suflita, D. R. Lovley, and L. Y. Young (1997), "Anaerobic degradation of benzene in diverse anoxic environments," *Environmental Science and Technology* **31**(3), 813–818.
- Lovley, D. R., M. J. Baedecker, D. J. Lonergan, I. M. Cozzarelli, E. J. P. Phillips, and D. I. Siegel (1989), "Oxidation of aromatic contaminants coupled to microbial iron reduction," *Nature* **339**(5), 297–300.
- Mace, R. E., R. S. Fisher, D. M. Welch, and S. P. Parra (1997), "Extent, Mass, and Duration of Hydrocarbon Petroleum Storage Tank Sites in Texas" *Bureau of Economic Geology*, University of Texas at Austin.

- MacIntyre, W. G., M. Boggs, C. P. Antworth, and T. B. Stauffer (1993), "Degradation kinetics of aromatic organic solutes introduced into a heterogeneous aquifer," *Water Resources Research* **20**(12), 4045–4051.
- Major, D. W., C. I. Mayfield, and J. F. Barker (1988), "Biotransformation of benzene by denitrification in aquifer sand," *Ground Water* **26**(1), 8–14.
- Parsons Engineering Science (1996), "Final Treatability Study to Evaluate Intrinsic Remediation at the North and South Gas Stations," Travis Air Force Base, California, Prepared for the Air Force Center for Environmental Excellence, Brooks Air Force Base, Texas.
- Press, W. H., S. A. Teukolsky, W. T. Vetterling, B. P. Flannery (1992), "Numerical Recipes in FORTRAN," (2nd Edition) (Cambridge University Press, New York).
- Rafai, H. S., P. B. Bedient, J. T. Wilson, K. M. Miller, and J. M. Armstrong (1987), "Biodegradation modeling at aviation fuel spill site," *Journal of Environmental Engineering, American Society of Civil Engineers* **114**(5), 1007–1029.
- Reinhard, M., N. L. Goodman, and J.F. Barker (1984), "Occurrence and distribution of organic chemicals in two landfill leachate plumes," *Environmental Science and Technology* **18**(12), 953–961.
- Rice, D. W., R. D. Grose, J. C. Michaelson, B. P. Dooher, D. H. MacQueen, S. J. Cullen, W. E. Kastenber, L. E. Everett, and M. A. Marino (1995), "California Leaking Underground Fuel Tank (LUFT) Historical Case Analyses," Lawrence Livermore National Laboratory, Livermore, Calif. (UCRL-AR-122207).
- Vroblesky, D. A., and F. H. Chapelle (1994), "Temporal and spatial changes of terminal electron-accepting processes in a petroleum hydrocarbon-contaminated aquifer and the significance for contaminant biodegradation," *Water Resources Research* **30**(5), 1561–1570.
- Vroblesky, D. A., P. M. Bradley, and F. H. Chapelle (1996), "Influence of electron donor on the minimum sulfate concentration required for sulfate reduction in a petroleum hydrocarbon-contaminated aquifer," *Environmental Science and Technology* **30**(4), 1377–1381.
- Wilson, J. L., and P. G. Miller (1978), "Two-dimensional plume in uniform ground-water flow," *Journal of the Hydraulics Division, in Proceedings of the American Society of Civil Engineers* **104**(4), 503–514.
- Wilson, J. T., G. Sewell, D. Caron, G. Doyle, and R. N. Miller (1995), "Intrinsic bioremediation of jet fuel contamination at George Air Force Base", in *Intrinsic Bioremediation*, Hinchee, R.E., J. T. Wilson, and D.C. Downey, Eds. (Battelle Press, Richland, Washington), pp. 91–100.
- Woodbury, A., F. Render, and T. Ulrych (1995), "Practical probabilistic groundwater modeling," *Ground Water* **33**(4), 532–538.

Table E-2.1. Median geochemical indicator concentrations in background wells (BTEX not detected) and plume interior wells (BTEX present above detection limit).

Indicator	Background (mg/L)	Plume interior (mg/L)
O ₂	0.5	0.2
Fe(II)	0.03	2.8
Mn ²⁺	0.1	2.8
NO ₃ ⁻	4.9	0.95
SO ₄ ²⁻	876	530
CH ₄	0.0045	0.16
HCO ₃ ⁻	393	746

Table E-2.2. Parameter values for two model realizations of the NSGS plume.

Parameter	Realization #1	Realization #2
Total mass per gas station (liters of gasoline)	103,700	51,800
Total mass per gas station [*] , M (grams of BTEX)	8.30 x 10 ⁶	4.15 x 10 ⁶
Length of release period, t (years)	20	20
First-order degradation rate, λ (day ⁻¹)	0.2%	0.05%
Hydraulic conductivity [†] (m/day)	4	4
Hydraulic gradient magnitude	0.002	0.002
Gradient direction (degrees)	295	295
Effective porosity [‡] , ϕ	0.2	0.2
Soil organic carbon [§] (mg/Kg)	1,600	1,600
Soil bulk density, ρ_b (g/cm ³)	1.65	1.65
Aquifer thickness, H (m)	3	3
Ratio of α_l to plume length scale ^{**}	0.1	0.05

* Assuming BTEX volume is equal to 10% of total gasoline volume; BTEX density = 0.8 g/cm³. M is introduced at a uniform rate into the system over the time period t.

† Velocity, v, used in Eq. (2) calculated from Darcy's law and porosity value.

‡ Total porosity is assumed to be equal to 1.5 times the effective porosity for calculation of the retardation coefficient.

§ Retardation coefficient, R, used in Eq. (2) calculated from the relationship $R = 1 + K_{oc}f_{oc}\rho_b/\phi$, where f_{oc} is the fractional organic carbon content of the sediments and K_{oc} , the organic carbon partitioning coefficient, is assumed to be equal to 280 ml/g as a representative value for BTEX.

** Dispersion coefficients, D_l and D_t , calculated by $D_l = v\alpha_l$ and $D_t = v\alpha_t$, where α_l and α_t are the longitudinal and transverse dispersivities, respectively. Plume length scale is given by vt .

Table E-2.2. (Continued)

Parameter	Realization #1	Realization #2
Ratio of α_t to α_1	0.1	0.025
Background SO_4^{2-} (mg/L)	876	876
Background HCO_3^- (mg/L)	390	390

Table E-2.3. Probability distributions of transport parameters used in Monte Carlo model.

Parameter	Distribution *	Rationale
Total mass per gas station (liters of gasoline)	Lognormal distribution. 5% = 51,850 95% = 207,400 Median = 73,100	Postulated.
Source locations, both gas stations (m)	Normal distribution. Tank location \pm 7.6 (N/S and E/W)	Postulated (accounting for leaks in piping systems, free product pools).
Release period, t (years)	Normal distribution; 20 ± 2 .	Based on tank use history.
First-order degradation rate, λ (day ⁻¹)	Lognormal distribution. 5% = 0.05% 95% = 1.0% Median = 0.2%	Postulated, based on reported values for mean degradation rates at other LUFT sites (e.g., MacIntyre et al., 1993, Wilson et al., 1995, Buscheck et al., 1996, Chapelle et al., 1996).
Hydraulic conductivity (m/day)	Lognormal distribution. 5% = 1 95% = 10 Median = 3.2	Based on site aquifer test data.
Hydraulic gradient	Lognormal distribution. 5% = 0.001 95% = 0.004 Median = 0.002	Based on a distribution of gradients obtained from trios of site wells.
Gradient direction (degrees)	Normal distribution; 295 ± 10 .	Based on observed spatial variability in NSGS gradient direction.
Effective porosity, ϕ	Normal distribution; 0.2 ± 0.02 .	Postulated.
Soil organic carbon (mg/Kg)	Weibull distribution. Loc = 367 Scale = 693 Shape = 1.36	Best-fit probability function to analyses of NSGS soil samples.
Bulk density, ρ_b (g/cm ³)	Normal distribution; 1.65 ± 0.02 .	Postulated.
Aquifer thickness, H (m)	Normal distribution; 10 ± 1 .	Based on site data.
Ratio of α_t to plume length scale	Lognormal distribution. 5% = 0.03 95% = 0.33 Median = 0.1	Postulated.
Ratio of α_t to α_l	Lognormal distribution.	Postulated.

* Uncertainty indicated in normal probability distributions refers to standard deviation.

Table E-2.3. (Continued)

Parameter	Distribution [†]	Rationale
SO ₄ ²⁻	5% = 0.03	Best-fit probability function. Correlated with alkalinity by analysis of monitoring well data (R = 0.67).
	95% = 0.33	
	Median = 0.1	
	Exponential distribution. Rate = 7.19 x 10 ⁻⁴	
Alkalinity [†]	Lognormal distribution.	Best-fit probability function. Correlated with SO ₄ ²⁻ .
	5% = 106	
	95% = 872	
	Median = 304	

[†] Measured alkalinity values converted to HCO₃⁻ to model reaction stoichiometry.

Table E-2.4. Sensitivity of select forecast geochemical indicator concentrations to model parameters.

Parameter well	SO42-		Bicarbonate		CH4	O2
	MW-138	MP-7	MW-138	MP-7	MW-138	MP-7
Background SO42-	54%	69%	5%	29%	31%	<1%
Background HCO3-	22%	30%	18%	67%	13%	<1%
Total mass per gas station	5%	<1%	8%	<1%	8%	<1%
Easting (South Gas Station source)	5%	<1%	27%	<1%	17%	<1%
Hydraulic conductivity	4%	<1%	14%	1%	9%	51%
Hydraulic gradient direction	2%	<1%	11%	<1%	6%	<1%
Ratio of t to l	2%	<1%	2%	<1%	3%	<1%
Hydraulic gradient magnitude	2%	<1%	3%	<1%	3%	14%
Northing (South Gas Station source)	1%	<1%	4%	<1%	3%	<1%
Ratio of l to plume length scale	1%	<1%	1%	<1%	1%	7%
Length of release period (time)	1%	<1%	1%	<1%	2%	<1%
Soil organic carbon	<1%	<1%	1%	<1%	1%	5%
First-order degradation rate	<1%	<1%	1%	<1%	<1%	<1%
Background dissolved O2	<1%	<1%	<1%	<1%	<1%	20%
Porosity	<1%	<1%	1%	1%	<1%	1%
Aquifer thickness	<1%	<1%	1%	<1%	1%	<1%
Others	1.50%	1%	2%	1%	1%	1%

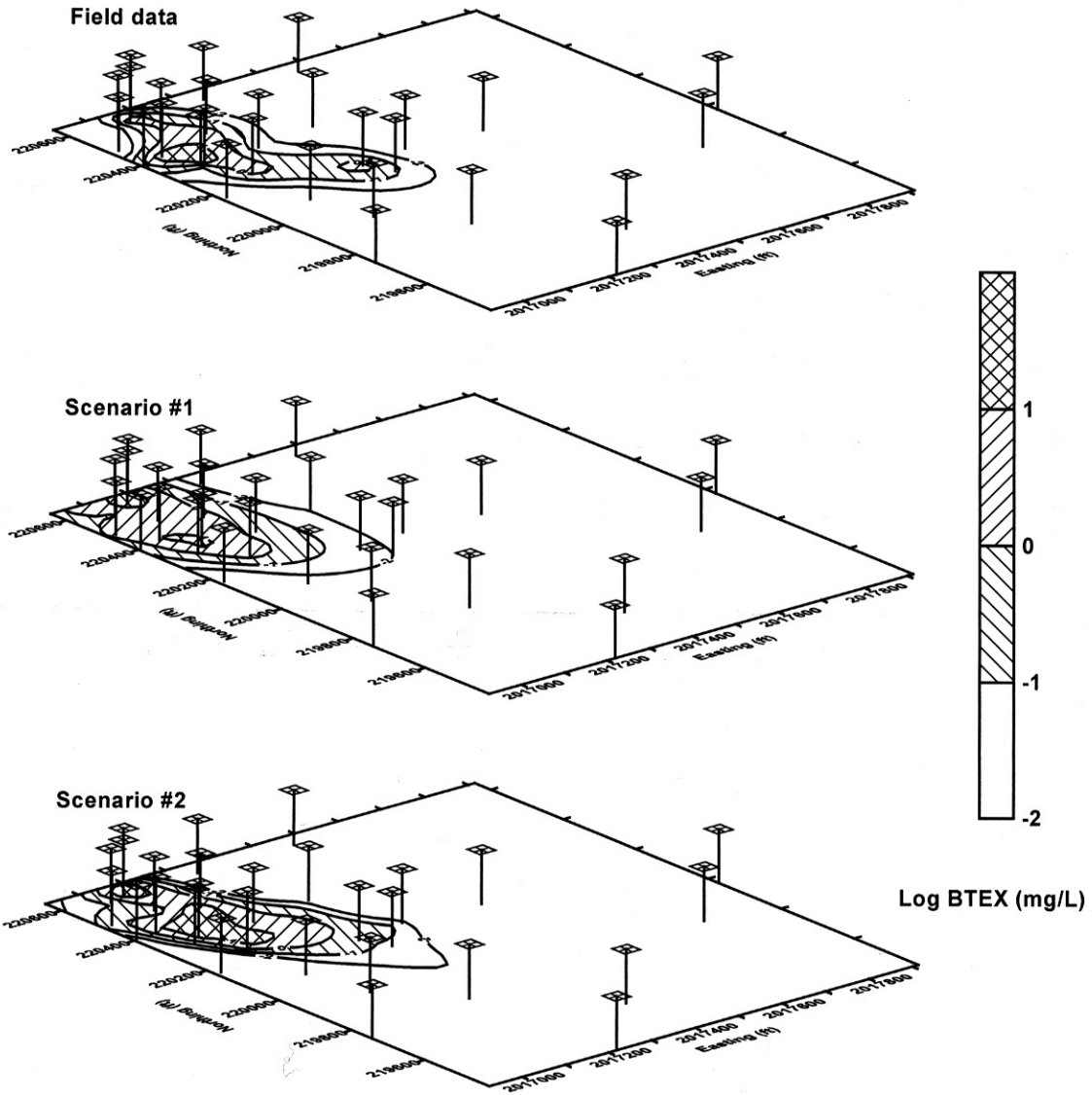


Fig. E-2.1. BTEX plume at the NSGS site (1995); field data (top), simulated Realization #1 (middle), and simulated Realization #2 (bottom). Units are logarithm of concentration (mg/L), contoured by monitoring well locations (hatched squares).

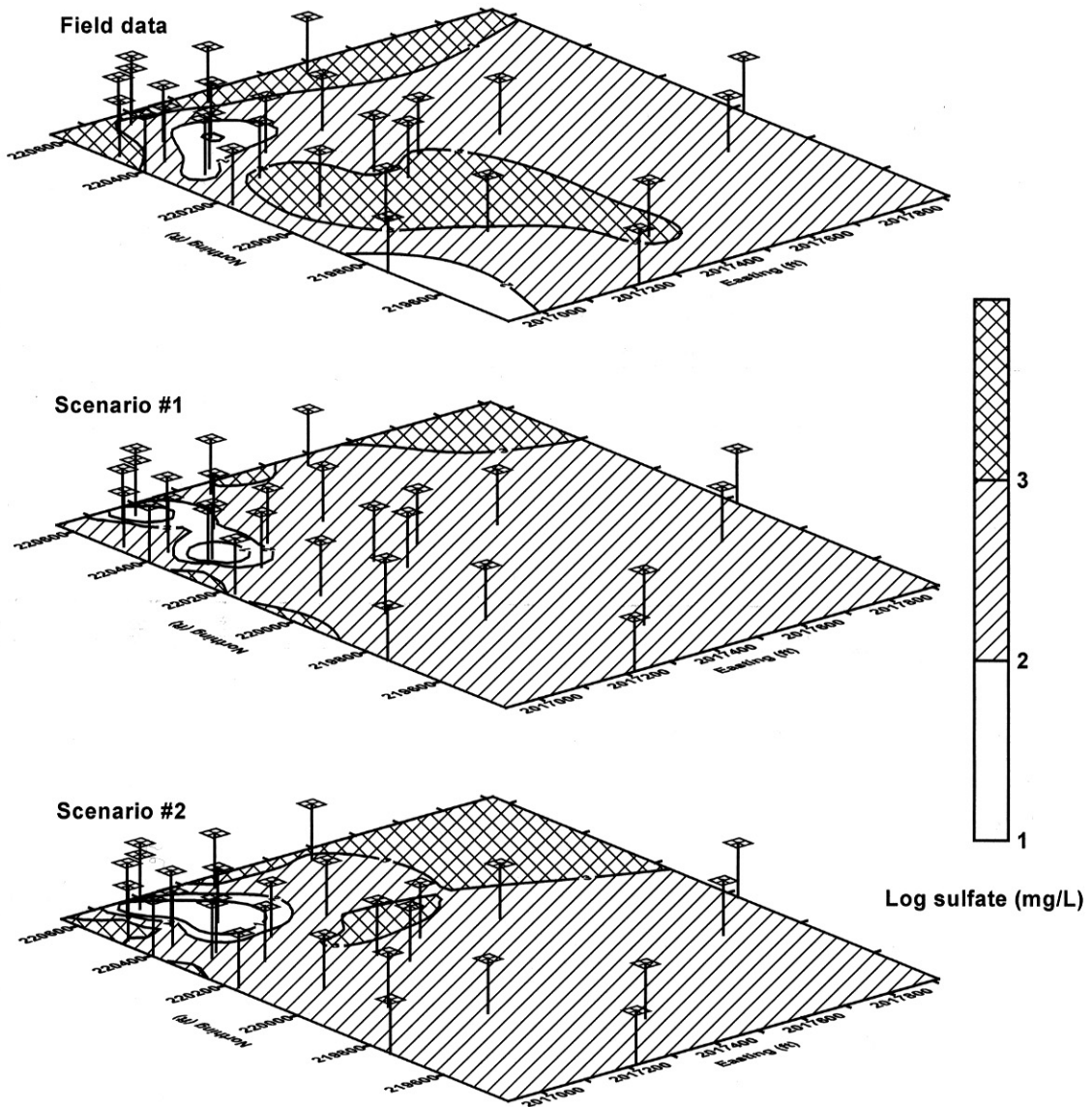


Fig. E-2.2. Distribution of sulfate in ground water at the NSGS site (1995); field data (top), simulated Realization #1 (middle), and simulated Realization #2 (bottom). Units are logarithm of concentration (mg/L), contoured by monitoring well locations (hatched squares).

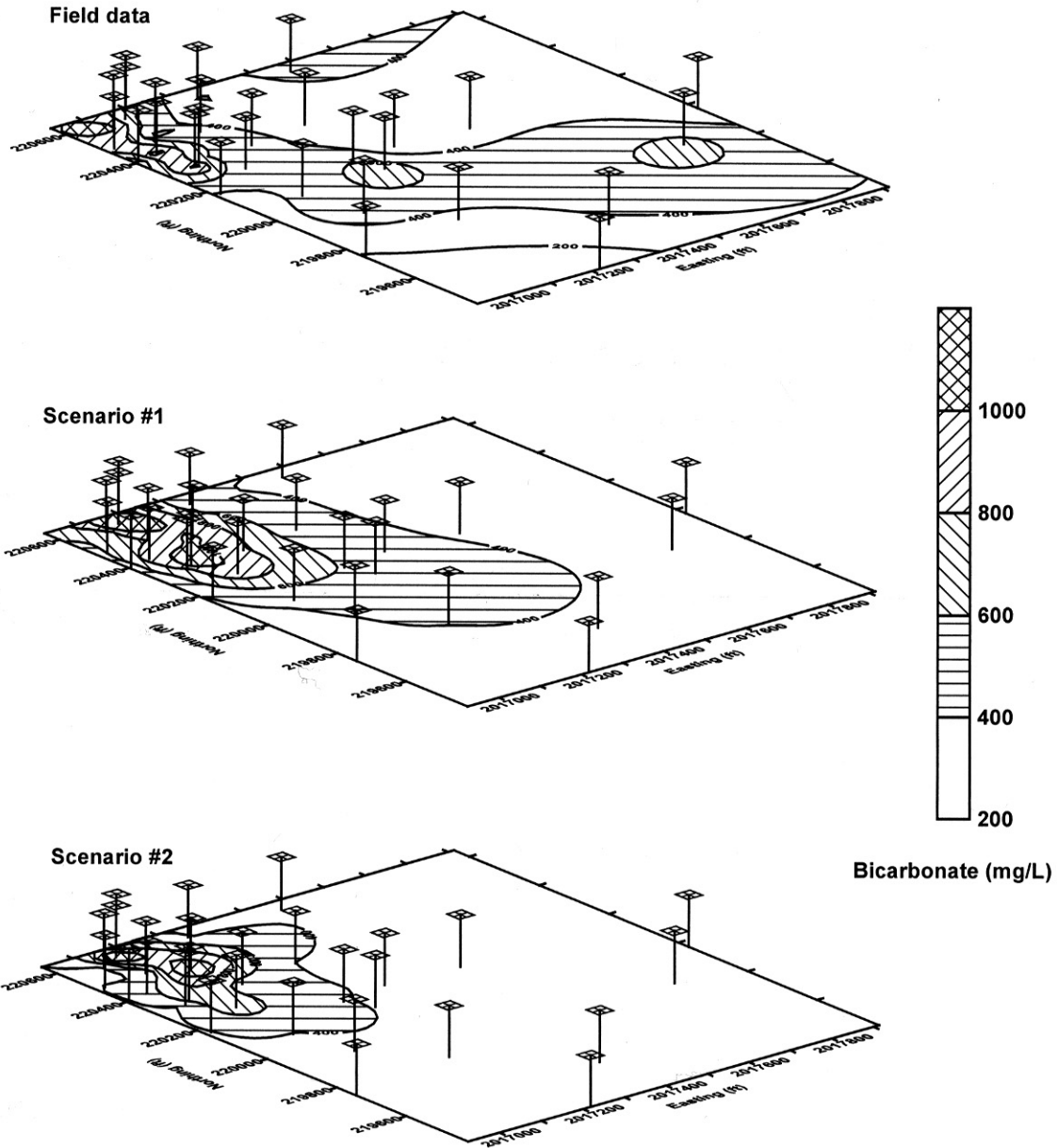


Fig. E-2.3. Distribution of bicarbonate in ground water at the NSGS site (1995); field data (top), simulated Realization #1 (middle), and simulated Realization #2 (bottom). Concentration units are mg/L, contoured by monitoring well locations (hatched squares).

Appendix E
Section E-3

**A Critique of a Steady-State Analytical Method
for Estimating Contaminant Degradation Rates**

Appendix E (Section E-3)

A Critique of a Steady-State Analytical Method for Estimating Contaminant Degradation Rates

E-3.1. Introduction

Fuel hydrocarbons and other common organic contaminants are frequently subject to biotransformation processes in groundwater environments. If the rate of biotransformation of a given contaminant at a site is assumed to be uniform in time and space, then in the presence of a continuous source (e.g., a residual pool of free product), the plume associated with the dissolved contaminant will achieve a steady-state configuration. This occurs as a result of a mass balance between contaminant influx from the source (e.g., free-product dissolution) and contaminant loss through biotransformation reactions integrated across the spatial extent of the plume. Therefore, the contaminant biotransformation rate will play a major role in determining the spatial extent of a steady-state contaminant plume in the direction downgradient from the source.

Buscheck and Alcantar (1995) suggested that the steady-state distribution of contaminant concentrations downgradient of a continuous source can be used to estimate transformation rates. This rate information is very useful, for example, in the assessment of the transport of a contaminant between its source and a risk receptor and in determining the required corrective action. Assuming a first-order decay coefficient as an approximation for the biotransformation of the contaminant, Buscheck and Alcantar (1995) showed, for a one-dimensional idealization, that the degradation rate λ may be given by,

$$\lambda = \frac{v_c}{4\alpha_x} \left(\left[1 + 2\alpha_x \left(\frac{k}{v_x} \right) \right]^2 - 1 \right) \quad (\text{E-3-1})$$

where v_c is the contaminant velocity along the x-direction (adjusted for retardation), α_x the longitudinal dispersivity, k the overall attenuation rate (units of % time⁻¹), and v_x the groundwater linear velocity. The term k/v_x reflects the slope of a regression line fit to log contaminant concentration data as a function of distance along the plume centerline (units of length⁻¹). This technique is routinely used to estimate biotransformation rates of contaminants in groundwater (e.g., Ellis, 1996; Brown et al., 1997; Herrington et al., 1997; Westervelt et al., 1997). However, it must be recognized that a significant potential for misinterpretation of results exists in applying this method. Buscheck and Alcantar (1995) intended for the method to be an idealization, recognizing that additional work and investigation would be required in order to narrow the bounds of the probable degradation rates. The difficulty arises when dispersive processes (macroscale mechanical mixing and molecular diffusion) produce concentration distributions which, ideally, decline with distance from a continuous source as determined by an error function term (even in the absence of any solute degradation). In many instances, particularly when analyzing only a small

number of data points (i.e. monitoring wells), it is often possible to fit a straight line through log concentration versus distance data with a high degree of correlation even when biotransformation is insignificant or absent altogether. Therefore, it is possible to derive estimated biotransformation rates which are entirely spurious.

E-3.2. Analyses

E.3.2.1. Potential for Misapplication to Non-Transforming Contaminants

The method of Buscheck and Alcantar (1995) constitutes an inverse solution technique. Inverse solutions by their nature are particularly sensitive to the initial and boundary conditions associated with the problem. This sensitivity is increased through measurement and modeling errors. Mathematically, such problems are considered ill-posed due to a lack of uniqueness and stability resulting from small changes in the input data. The potential for misinterpretation of the inverse problem through application of the Buscheck and Alcantar (1995) method is best illustrated by an example problem. Consider the total BTEX (benzene/toluene/ethylbenzene/xylene) concentrations measured in three monitoring wells located downgradient of a leaking underground fuel tank (LUFT) site in northern California which is under consideration for remediation by natural attenuation (Table E-3.1). Mean hydraulic conductivity in monitoring wells across the site, estimated from slug tests and pumping tests, is approximately 3.6 m/day. Assuming a hydraulic gradient of 0.002, an effective porosity of 0.25, and a retardation coefficient of approximately 2.0 (based on soil organic carbon content and organic carbon partitioning properties of BTEX), a retarded contaminant velocity of approximately 5.2 m/year may be estimated. Given the length of the BTEX plume at the site, approximately 150 meters based on the 10 $\mu\text{g/L}$ contour, longitudinal dispersivity (characteristic length) may be estimated from the relationship given by Neumann and Zhang (1990),

$$\alpha_x = 0.32L^{0.83} \quad (\text{E-3-2})$$

where L is the scale of the plume length, or simply by assuming a characteristic length equal to 0.10 of the plume length (20 m or 15 m, respectively). Linear regression of log BTEX concentrations as a function of distance from the source area yields a k/v_x value of 0.023, with $R^2 = 0.974$ (Fig. E-3.1). Substitution of this k/v_x value in Eq. (E-3-1) yields biotransformations rate estimates of 0.048% day^{-1} and 0.045% day^{-1} for the Neumann and Zhang and 0.10L dispersion relationships, respectively.

Now consider an alternate scenario. Suppose that the BTEX plume at the site behaves ideally and may be modeled using the familiar Domenico (1987) solution to the two-dimensional advective-dispersive transport equation with a continuous line source,

$$C(x, y, t) = \left(\frac{C_0}{4} \right) \exp \left\{ \left[\frac{x}{2\alpha_x} \right] \left[1 - \left(1 + \frac{4R\lambda\alpha_x}{v} \right)^{1/2} \right] \right\} \\ \cdot \operatorname{erfc} \left[\frac{x - \frac{v}{R}t \left(1 + 4R\lambda\alpha_x / v \right)^{1/2}}{2 \left(\alpha_x \frac{v}{R}t \right)^{1/2}} \right] \cdot \left\{ \operatorname{erf} \left[\frac{(y + Y/2)}{2(\alpha_y x)^{1/2}} \right] - \operatorname{erf} \left[\frac{(y - Y/2)}{2(\alpha_y x)^{1/2}} \right] \right\} \quad (\text{E-3-3})$$

Here, C_0 refers to the source concentration (constant with time), α_y the transverse dispersivity, v the groundwater pore velocity, R the retardation coefficient, Y the width of the line source, t the monitor time, and x and y the Cartesian coordinates of the monitor point relative to the source. Assuming a value of 67,000 $\mu\text{g/l}$ for C_0 , a source width of 15 m, a flow velocity of 10.4 m/year (corresponding to a contaminant velocity of 5.2 m/year when $R = 2.0$), and a non-transforming tracer ($\lambda = 0.0$), modeled concentrations as a function of distance may be generated for a variety of longitudinal and transverse dispersivity combinations (Figs. E-3.2 and E-3.3). Given that the Domenico (1987) relationship constitutes a mathematical physical model of solute transport processes, the forecast observations are entirely plausible in that they could, in principle, depict the behavior of a real plume to an observer. For all scenarios chosen, the modeled results resemble the field observations in that log concentration apparently varies linearly with distance from the source. As a result, entirely spurious biotransformation rates can be calculated from Eq. (E-3-1) in the absence of any corroborating information (Table E-3.2), with the highest implied rates corresponding to smaller values of α_x and larger values of α_y .

This example illustrates the potential for misinterpretation of contaminant degradation by the Buscheck and Alcantar (1995) method even under ideal conditions. A linear trend in log concentration values as a function of distance from the contaminant source does not constitute proof of the existence of transformation processes. In particular, it should also be recognized that utilizing only a small number of monitoring wells increases the chances for misinterpretation because of the high probability of a spurious linear fit. For example, consider the results of the example scenario using 11 equidistant monitoring wells instead of three (Fig. E-3.4). The higher well density illustrates a departure from linearity in the log concentration versus distance relationship which was not observed when fewer wells were analyzed.

In reality, many other factors will distort observed concentration profiles in comparison to those predicted by idealized models. A partial list includes (1) the assumption of steady-state conditions where none exist, (2) fluctuations in source strength with time, (3) non-Fickian dispersion of solutes, (4) strongly heterogeneous flow and transport, (5) placement of wells off plume centerline, (6) dilution effects due to well screen length, and (7) non-uniform degradation rate distribution. Thus, fitting concentration data with an exponential function is perhaps simply a matter of chance in many situations, particularly when few monitoring points are utilized, and thus may provide little real insight into transformation processes.

E-3.3. Sensitivity Analyses

Sensitivity analyses provide a means for assessing which parameters exert the greatest influence on the results of the Buscheck and Alcantar method. One approach at addressing the

sensitivity issue is to again utilize an idealized model such as the Domenico solution to generate a large number of synthetic BTEX plumes through Monte Carlo simulation, using a range of physical parameter values and biotransformation rates. Monte Carlo simulation is a method by which numbers are randomly drawn from a prescribed series of distributions. The use of Monte Carlo simulations combined with analytical methods results in an output that places confidence limits on the idealized model that can then be compared to the results of a real world situation (e.g., McNab and Dooher, 1998). A comparison of prescribed biotransformation rates in the input parameter probability distribution with inferred rates yielded by application of the Buscheck and Alcantar method to each realization may provide insight into the resulting error distribution. Sensitivity of this error distribution to the parameter input values may offer clues as to which situations are most amenable to the Buscheck and Alcantar method and which are less appropriate.

Hypothesized probability distributions for parameters which directly or indirectly feed into the Domenico relationship (Eq. E-3-3) are shown on Table E-3.3, again with reference to the northern California LUFT site (i.e., with three monitoring points). A total of 1000 realizations were conducted as part of the Monte Carlo simulation. Input for each realization consisted of model parameters chosen randomly in accordance with the probability distributions. Output consisted of forecast concentrations of total BTEX at the three monitoring points (Table E-3.1). Linear regression was performed on the log BTEX concentration versus distance output to produce k/v_x values for input into the Buscheck and Alcantar equation.

Monte Carlo realizations were performed using commercial spreadsheet software. The correlation coefficient relating log total BTEX concentrations and distance was greater than 0.97 in 90% of the realizations, indicating that the Buscheck and Alcantar approach could be applied, in principle, to the vast majority of the cases. Forecast probability (cumulative) distributions of prescribed biotransformation rates as well as the rates derived from the Buscheck and Alcantar approach are illustrated on Fig. E-3.5. These results suggest a significant potential for systematic overestimation of biotransformation rates. This is not surprising, given that the contribution of dispersion in influencing the longitudinal profile of the plume.

A measure of the biotransformation rate estimation error, on a per realization basis, may be given as,

$$\text{Error} = (\lambda_{\text{prescribed}} - \lambda_{\text{B-A}})^2 \quad (\text{E-3-4})$$

where $\lambda_{\text{prescribed}}$ refers to the specified bioattenuation rate and $\lambda_{\text{B-A}}$ the bioattenuation rate derived from application of the Buscheck and Alcantar technique. Sensitivity analysis of this defined error function to the input parameters was calculated by rank correlation to avoid the skewing effects of nonlinear relationships between model input and output. The resulting correlation coefficients are shown on Fig. E-3.6. Elapsed time since the initiation of the source appears to be the most significant factor influencing the accuracy of the Buscheck and Alcantar method in this example, with the negative correlation coefficient ($R = -0.79$) suggesting the greatest error at earliest in the plume history. This is to be expected, as the plume profile will not have had time to stabilize during its initial stages because of the time required for degrading plumes to reach their maximum extent and the rapid growth associated with young plumes. Of secondary influence is the variability associated with dispersion, the velocity-based components of gradient and hydraulic

conductivity, and the source width. Thus, the fall-off in concentration with distance is entirely associated with source descriptions and physical transport processes. It is not surprising then that the variability associated with terms that are very uncertain or sparsely sampled to begin with can have significant impact on how degradation rates are developed (Dooher, 1998).

The estimation error also correlates with the value of the derived biotransformation rate (not shown), with a correlation coefficient of +0.73. This suggests that the highest derived biotransformation rates yielded by the Buscheck and Alcantar analyses are the most strongly reflective of non-transformative processes.

E-3.4. Conclusions

The analyses presented in this study suggest that the Buscheck and Alcantar (1995) method for estimating *in situ* biotransformation rates may yield misleading results if not applied in a judicious manner. Buscheck and Alcantar were aware of the possible difficulties, but uncritical application of the method by many workers to groundwater contamination problems continues. Potential erroneous or even spurious transformation rates may arise because of the effects of dispersion in stable plumes as well as in plumes in early stages of development before steady-state is reached. In particular, the method may yield incorrect results when only a small number of wells are used, as the exponential regression will provide a better fit under such circumstances.

These findings imply that biotransformation rates yielded by the Buscheck and Alcantar method should always be substantiated. In principle, this should require that a sufficient number of monitoring wells should be chosen so that the linearity of the log concentration versus distance relationship be either established or refuted. However, in many instances a sufficient number of monitoring wells may be lacking. In such cases, independent means of quantifying transformation rates should be brought to bear. These may include alternate modeling tools such as more comprehensive analytical solute transport models (e.g., Cleary and Unga, 1978; Wilson and Miller, 1978; Domenico, 1987) or numerical approaches as warranted (Rafai et al., 1987). In addition, mass balance constraints implied by geochemical indicator parameters, such as dissolved oxygen, nitrate, sulfate, iron, bicarbonate, and methane may also providing supporting insights.

E-3.5. References

- Buscheck, T. E., and C. M. Alcantar (1995), "Regressive techniques and analytical solutions to demonstrate intrinsic bioremediation," in *Intrinsic Bioremediation*, R. E. Hinchee, J. T. Wilson, and D. Downey, Eds. (Battelle Press, Columbus, Ohio) pp. 109–116.
- Brown, K. P. Sererka, M. Thomas, T. Perina, L. Tyner, and B. Sommer (1997), "Natural attenuation of Jet-Fuel Impacted Groundwater," in *In Situ and On-Site Bioremediation: Volume 1, Fourth International in Situ and On-Site Bioremediation Symposium*, New Orleans, April 28–May 1, pp. 83–88.
- Chapelle, F. H., P. M. Bradley, D. R. Lovley, and D. A. Vroblesky (1996), "Measuring rates of biodegradation in a contaminated aquifer using field and laboratory methods," *Ground Water* **34**(4), 691–698.
- Cleary, R. W., and M. J. Unga (1978), "Groundwater pollution and hydrology, mathematical models and computer programs," Report 78-WR-15, Water Resources Program, Princeton University, Princeton, New Jersey.
- Domenico, P. A. (1987), "An analytical model for multidimensional transport of a decaying contaminant species," *Journal of Hydrology* **91**, 49–58.
- Dooher, B. P. (1998), "Making risk-based decisions at fuel hydrocarbon impacted sites under sparse data conditions," Ph.D. Dissertation, University of Calif., Los Angeles.
- Ellis, D. E. (1996), "Intrinsic remediation in the industrial marketplace," in *Symposium on Natural Attenuation of Chlorinated Organics in Ground Water*, Dallas, Texas, September 11–13, (EPA/540/R-96/509), pp. 120–123.
- Herrington, R. T., L. Benson, D. Downey, and J. Hansen (1997), "Validation of fuel hydrocarbon attenuation in low-temperature groundwater environments," in *In Situ and On-Site Bioremediation: Volume 1, Fourth International in Situ and On-Site Bioremediation Symposium*, New Orleans, April 28–May 1, pp. 303–308.
- MacIntyre, W. G., M. Boggs, C. P. Antworth, and T. B. Stauffer (1993), "Degradation kinetics of aromatic organic solutes introduced into a heterogeneous aquifer," *Water Resources Research* **20**, 4045–4051.
- McNab, W. W., Jr., and B. P. Dooher (1998), "Uncertainty analyses of fuel hydrocarbon biodegradation signatures in ground water by probabilistic modeling," *Ground Water*, **36**(4), 691–698.
- Neumann, S. P., and Y.-K.Zhang (1990), "A quasi-linear theory of non-Fickian and Fickian subsurface dispersion **1**, Theoretical analysis with application to isotropic media," *Water Resources Research* **26**(5), 887–902.
- Rafai, H. S., P. B. Bedient, J. T. Wilson, K. M. Miller, and J. M. Armstrong (1987), "Biodegradation modeling at aviation fuel spill site," *Journal of Environmental Engineering*, American Society of Civil Engineers **114**(5), 1007–1029.

- Wilson, J. L., and P. G. Miller (1978), "Two-dimensional plume in uniform ground-water flow," *Journal of the Hydraulics Division*, in *Proceedings of the American Society of Civil Engineers* **104**, pp. 503–514.
- Westervelt, W. W., P. W. Lawson, M. N. Wallace, and C. Fosbrook (1997), "Intrinsic remediation of arctic diesel fuel near drinking water wells," in *In Situ and On-Site Bioremediation: Volume 1, Fourth International In Situ and On-Site Bioremediation Symposium*, New Orleans, April 28–May 1, pp. 61–66.
- Wilson, J. T., G. Sewell, D. Caron, G. Doyle, and R. N. Miller (1995), "Intrinsic Bioremediation of Jet Fuel Contamination at George Air Force Base," in *Intrinsic Bioremediation*, Hinchee, R. E., J. T. Wilson, and D. C. Downey, Eds. (Battelle Press, Richland, Washington), pp. 91–100.

Table E-3.1. BTEX concentrations as a function of distance from source.

Well	Distance downgradient (m)	Total BTEX ($\mu\text{g/l}$)
Well #1	0	67,000
Well #2	26	23,500
Well #3	113	4,095

Table E-3.2. Inferred biotransformation rates from analysis of BTEX concentrations idealized by the Domenico (1987) model.

α_x (m)	α_y (m)	R^2	k/v_x (m^{-1})	Inferred λ (day^{-1})
5	1	0.9845	0.0342	0.058%
10	1	0.9938	0.0263	0.048%
15	1	0.9975	0.0231	0.045%
20	1	0.9991	0.0212	0.043%
5	2.5	0.9975	0.0373	0.064%
10	2.5	0.9999	0.0294	0.055%
15	2.5	0.9976	0.0261	0.052%
20	2.5	0.9945	0.0243	0.052%

Table E-3.3. Probability distributions of parameters used in Monte Carlo model.

Parameter	Distribution	Rationale
Width of source (m)	Lognormal distribution. 5% = 1 95% = 25 Median = 5	Postulated.
Length of release period, t (days)	Lognormal distribution. 5% = 1000 95% = 10,000 Median = 3150	Postulated.
First-order degradation rate, λ (day ⁻¹)	Lognormal distribution. 5% = 0.05% 95% = 1.0% Median = 0.2%	Postulated, based on reported values for mean first-order degradation constants at other LUFT sites (e.g., MacIntyre et al., 1993, Wilson et al., 1995, Chapelle et al., 1996).
Hydraulic conductivity ¹ (m/day)	Lognormal distribution. 5% = 1 95% = 10 Median = 3.2	Based on site data (slug tests, aquifer tests).
Hydraulic gradient magnitude	Lognormal distribution. 5% = 0.001 95% = 0.004 Median = 0.002	Based on spatial variability in gradients observed at the site.
Porosity, ϕ	Normal distribution. 0.25 \pm 0.02	Postulated.
Retardation coefficient, R	Lognormal distribution. 5% = 1.5 95% = 5 Median = 2.7	Postulated.
Longitudinal dispersivity, α_x (m)	Lognormal distribution. 5% = 2 95% = 30 Median = 7.7	Postulated.
Transverse dispersivity, α_y (m)	Lognormal distribution. 5% = 0.2 95% = 3.0 Median = 0.8	Postulated.

¹Velocity term in the Domenico (1987) relationship estimated by application of Darcy's law to the prescribed hydraulic conductivity, gradient, and porosity.

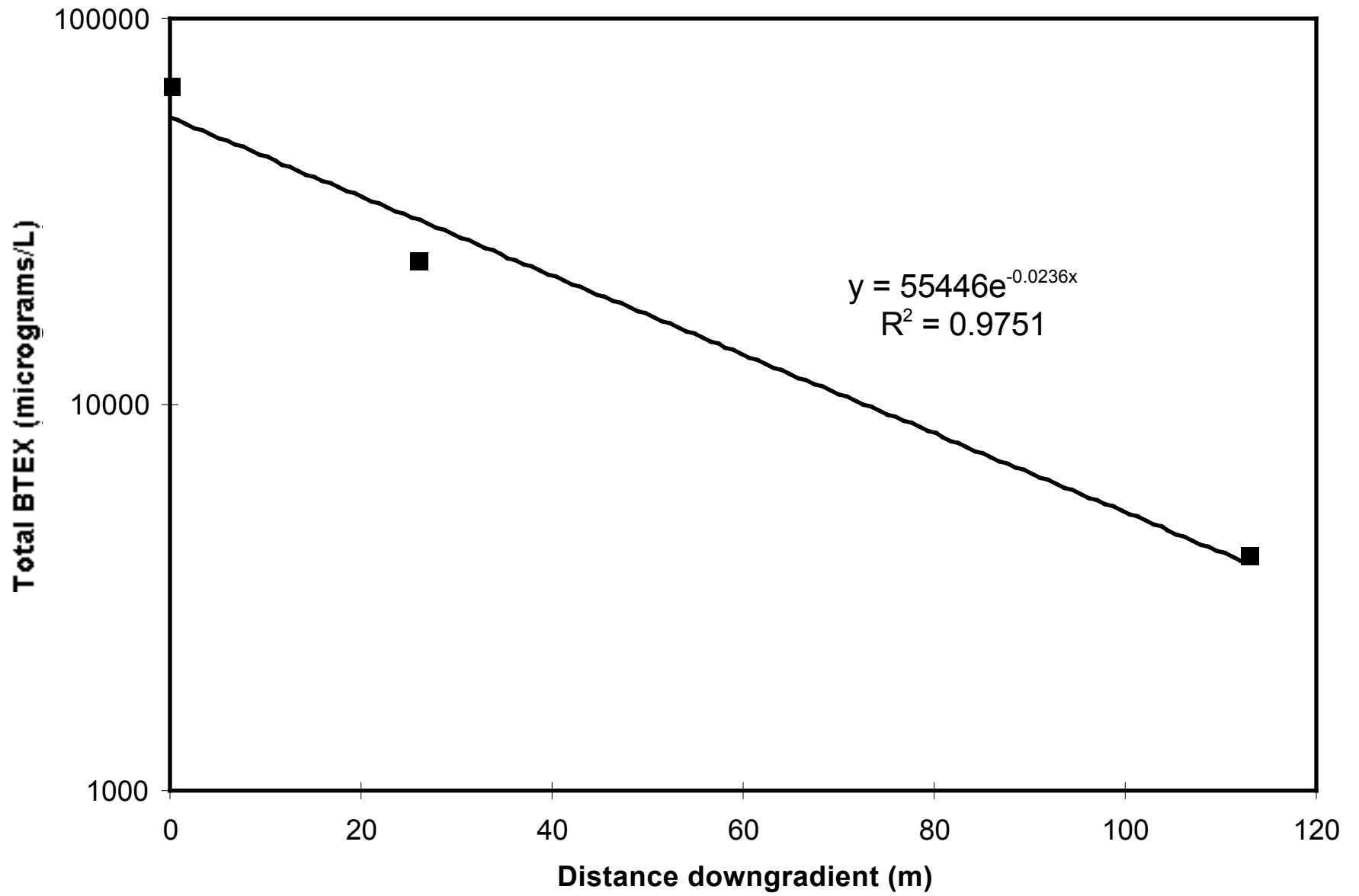


Figure E-3.1. Concentration versus distance downgradient (site data) used in analysis by the method of Buscheck and Alcantar (1995).

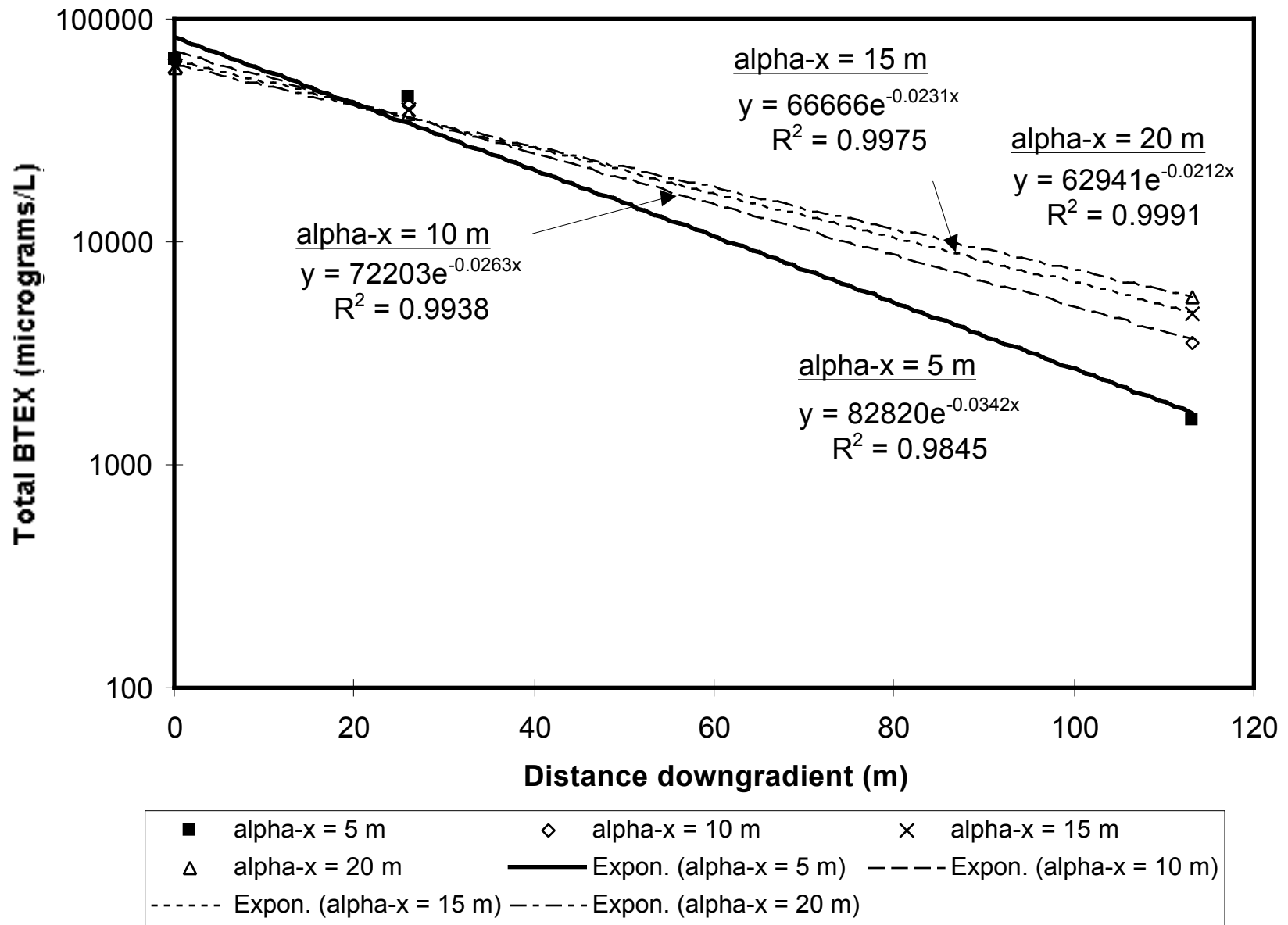


Figure E-3.2. Idealized Domenico (1987) model of concentration versus distance downgradient from source without degradation: Elapsed time = 5000 days, $\alpha_y = 1 \text{ m}$.

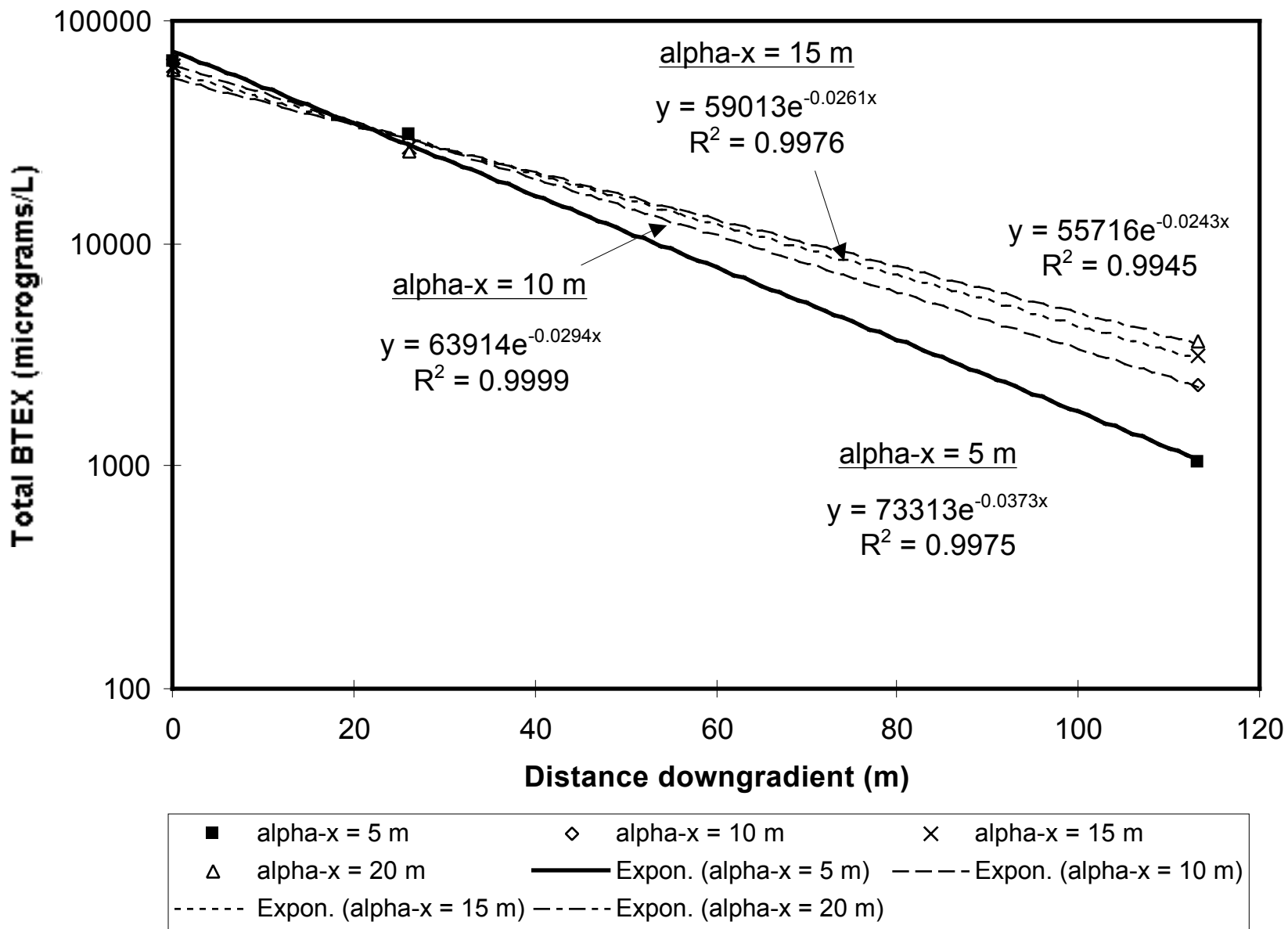


Figure E-3.3. Idealized Domenico (1987) model of concentration versus distance downgradient form source without degradation: Elapsed time = 5000 days, $\alpha_y = 2.5$ m.

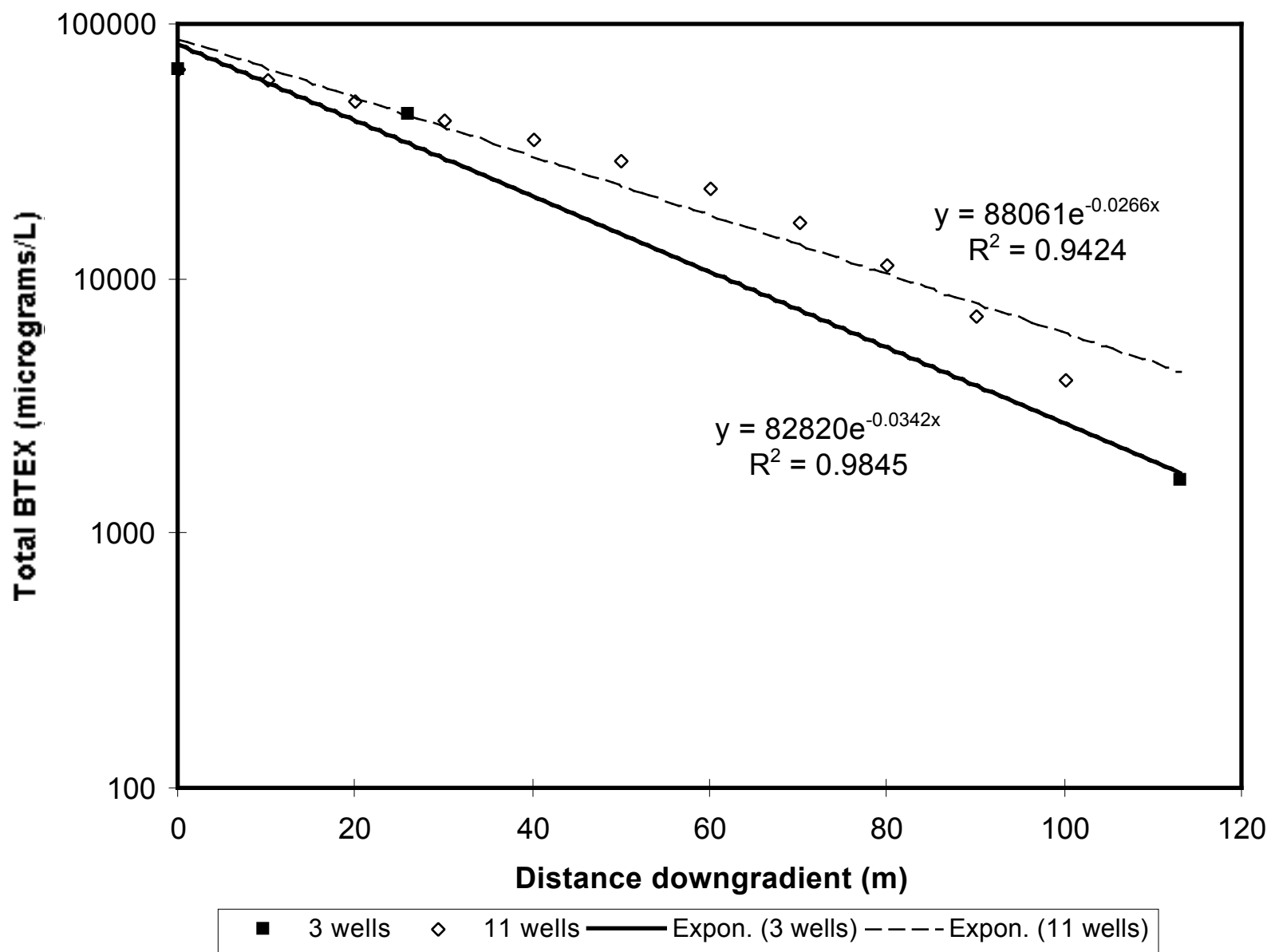


Figure E-3.4. Idealized Domenico (1987) model of concentration versus distance downgradient from source without degradation: Elapsed time = 5000 days, $\alpha_x = 5$ m, $\alpha_y = 1$ m.

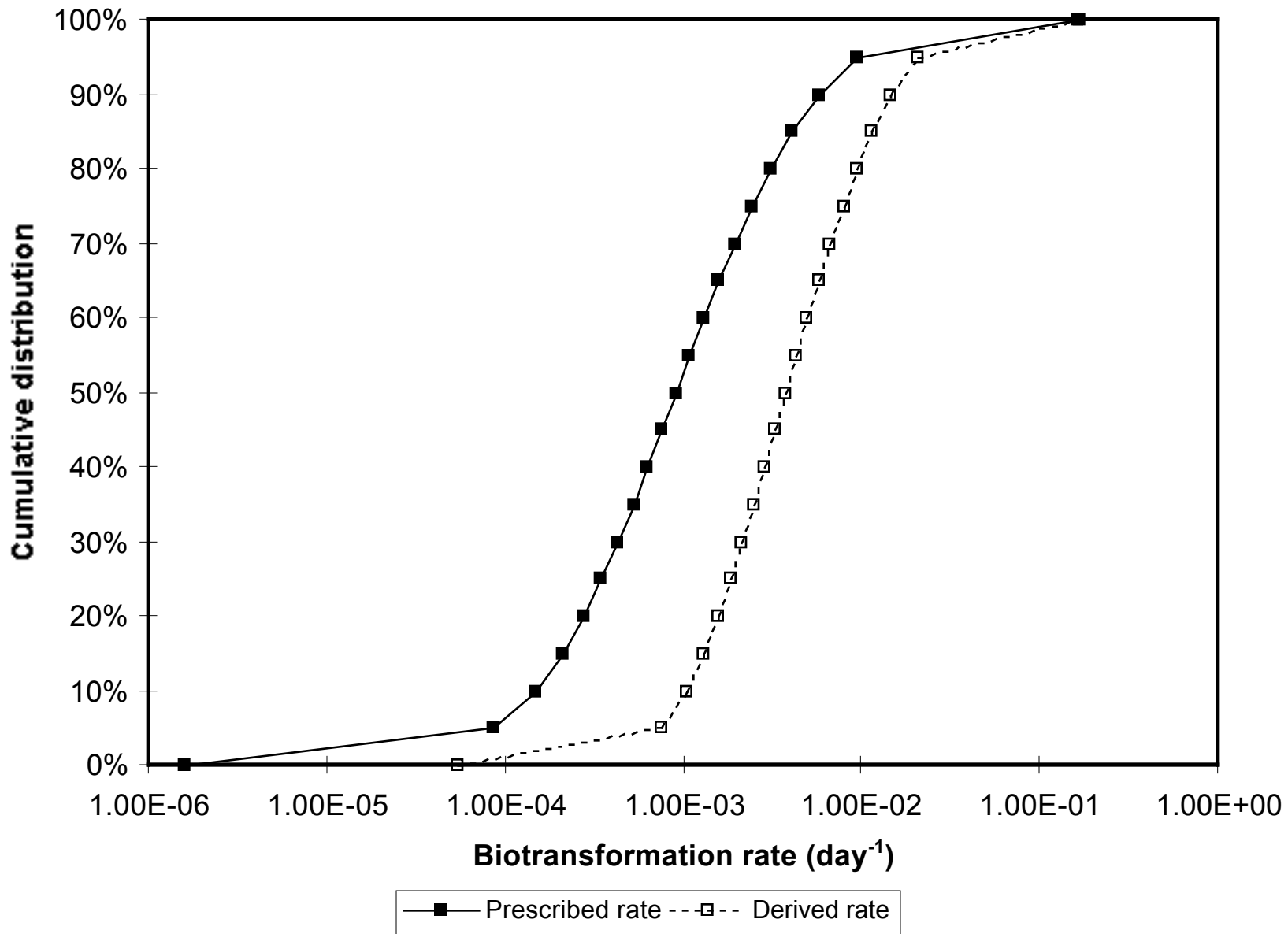


Figure E-3.5. Cumulative distribution of prescribed (input) and derived (output) BTEX biotransformation rates.

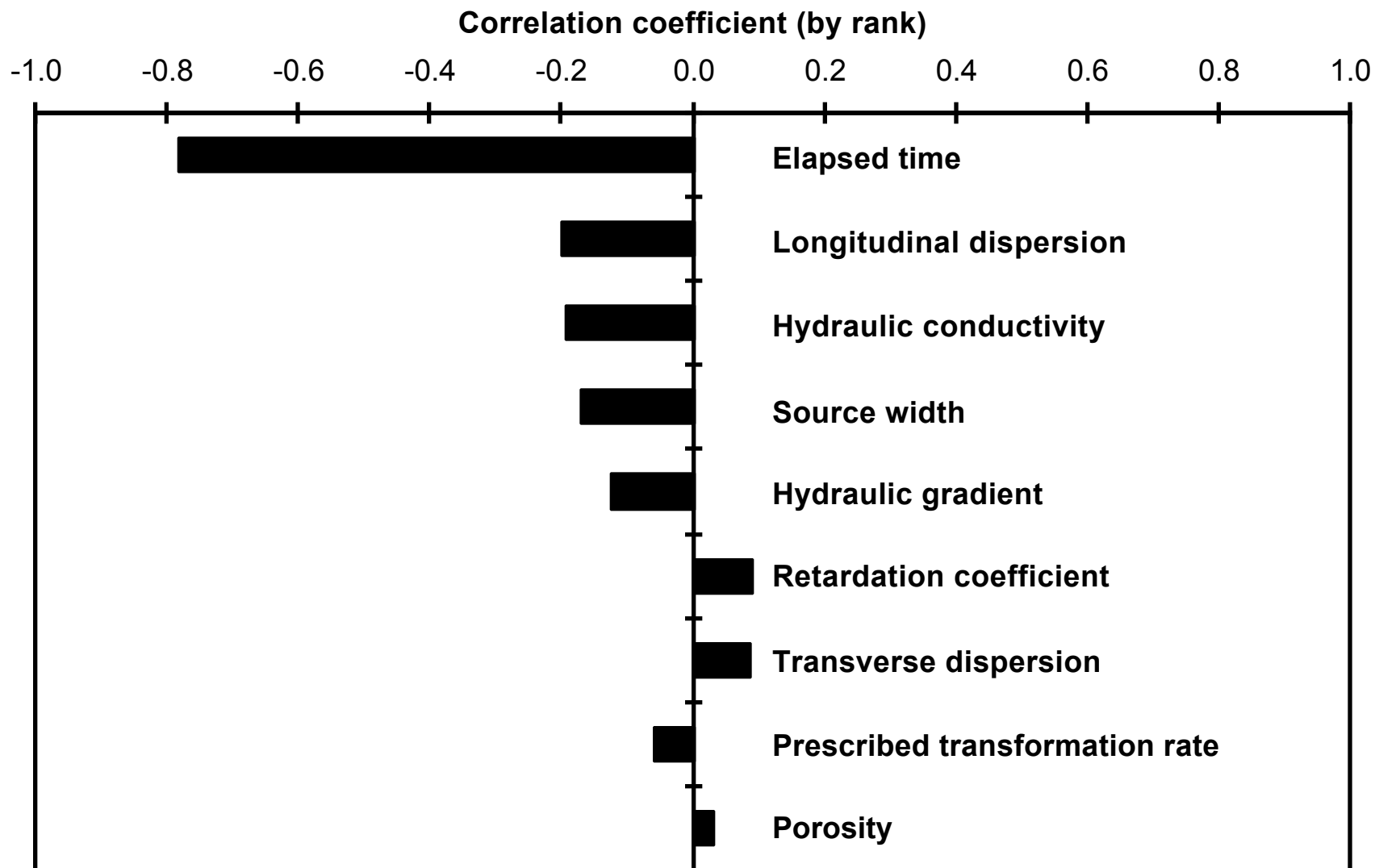


Figure E-3.6. Correlation of estimation error (by rank) with Monte Carlo input parameters.

Appendix E
Section E-4

**Estimation of Fuel Hydrocarbon Biodegradation
Rates by Integrated Analysis of Plume Lengths
and Bicarbonate Alkalinity**

Appendix E (Section E-4)

Estimation of Fuel Hydrocarbon Biodegradation Rates by Integrated Analyses of Plume Lengths and Bicarbonate Alkalinity

E-4.1. Introduction

Dissolved fuel hydrocarbons associated with leaking underground fuel tanks (LUFTs) are known to biodegrade in groundwater under a variety of biogeochemical regimes [Reinhard et al., 1984; Barker et al., 1987; Major et al., 1988; Baedeker et al., 1993; Lovley et al., 1995; Kazumi et al., 1997]. As such, groundwater hydrocarbon plumes may undergo some degree of self-remediation which may limit downgradient migration and hence reduce some of the associated exposure risks [Salanitro, 1993; Rice et al., 1995; Mace et al., 1997]. Even in the presence of a continuous source of fresh contaminants (e.g., from residual free-product lenses in the vadose zone), mass loss through biodegradation, integrated across the spatial extent of the plume, will eventually lead to a steady-state condition in terms of plume length. Clearly, the eventual downgradient extent of such a stable plume, a measure of the risk posed to receptors such as water supply wells, will depend on the overall rate of biodegradation. Moreover, the rate of biodegradation will also strongly influence the amount of time required to effectively remediate a site altogether once the contaminant source is removed. Therefore, a means for estimating mean biodegradation rates at LUFT sites, essentially an inverse problem, is important.

In general, hydrocarbon biodegradation rates are compound-specific and reflect local biogeochemical conditions within a plume (Vroblesky and Chapelle, 1994; Chapelle et al., 1996). Reaction rates have been modeled using Monod-type expressions, accounting for microbiological constraints on substrate utilization (Borden and Bedient, 1986). However, from a practical, field-oriented engineering perspective, a simple first-order kinetic model is often used in site investigations (Wilson et al., 1995; Buscheck et al., 1996). Two techniques are commonly employed to estimate mean first-order biodegradation rates at LUFT sites where the source release history is not well known. One method involves exponential regression of measured concentrations as a function of distance downgradient from the source area along the longitudinal axis of the plume (Buscheck and Alcantar, 1995). This method relies on an expected one-dimensional concentration profile of an ideal plume under steady-state conditions. Although this technique is widely used, the idealized profile is easily influenced by dispersive effects, creating the potential for significant error. A second method involves the normalization of concentrations of degradable hydrocarbon components (e.g., benzene, toluene) by those of presumably recalcitrant constituents, such as tri- and tetramethylbenzene isomers. Changes in the concentration ratios with distance from the source are, in principle, reflective of the rate of biodegradation of the degradable compound of interest. However, the recalcitrance of tri- and tetramethylbenzenes in the multiple biogeochemical zones typically associated with LUFT sites is uncertain (Herner et al., 1997), so the interpretation of biodegradation rates may be problematic.

The goal of this study is to develop estimates of hydrocarbon biodegradation rates using more direct indicators: limitation of plume length and differences in bicarbonate alkalinity between background and the plume interior (a reflection of hydrocarbon mineralization). The estimates are derived with respect to a population of plumes, rather than for an individual site, and thus are viewed from a probabilistic perspective.

E-4.2. Theory

Several factors will determine the spatial extent of an ideal dissolved hydrocarbon plume emanating from a specified solute flux source. These include mean groundwater velocity, the dispersion coefficients (reflecting the heterogeneous nature of the subsurface), the mean biodegradation rate, the nature of the source term, the retardation coefficient, the porosity, and the aquifer vertical thickness. If mean values were available for a population of LUFT sites and associated hydrocarbon plumes, some degree of inverse correlation would be expected between the mean biodegradation rate and plume length. The scatter in this relationship would reflect the contributions to variance associated with the other variables.

Over a large number of sites, the effects of site-specific features such as pronounced physical heterogeneities in the flow field will tend to average together and thus may be represented conceptually by a simple dispersion model. Thus, macro-scale plume features, such as plume length, may be modeled in a probabilistic sense using Monte Carlo simulation of analytical solutions to the advective-dispersive transport equation. If probability distributions of input variables other than the biodegradation rate are reasonably well-constrained, and if estimates of plume length based on field data from a number of sites can be used for comparison to forecast plume lengths, then a likely range of biodegradation rates which are consistent with observed plume lengths may be identified.

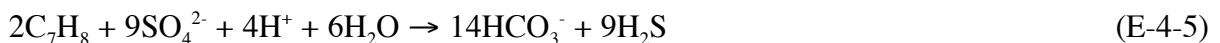
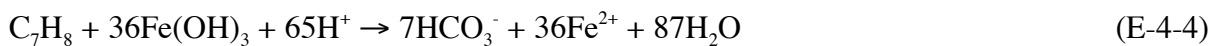
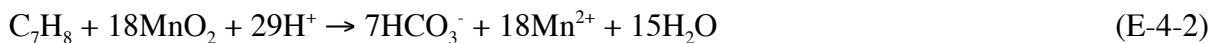
The effectiveness of using plume length distributions to constrain biodegradation rate distributions by Monte Carlo simulation will depend on two factors. The first is the overall applicability of analytical solutions for probabilistic modeling of groundwater plumes in terms of whether or not all essential features and processes are addressed. The second factor is the choice of probability distribution functions for input parameters (e.g., groundwater velocity, dispersion coefficients) which will obviously exert a major impact on simulation results regardless of the applicability of the analytical solution. To address these issues, a second, independent constraint may be called upon as a consistency check on the simulation results. The eventual end product of hydrocarbon mineralization is CO_2 , which combines with water to form carbonic acid, H_2CO_3 . In the near-neutral pH environments typically encountered in shallow, alluvial settings where LUFT sites are often found, H_2CO_3 will dissociate into bicarbonate, HCO_3^- , which is often measured in groundwater as bicarbonate alkalinity [Drever, 1988]. Indeed, bicarbonate alkalinity has been used a direct indicator of fuel hydrocarbon mineralization in groundwater (McNab and Doohar, 1998) **VERIFY YEAR**. Mass-balance constraints implied by reaction stoichiometry, combined with superposition of concentrations given by the analytical solution, permit the calculation of bicarbonate alkalinity values associated with a biodegrading hydrocarbon plume as a function of time and space. Thus, forecast differences in bicarbonate alkalinity between the interior of the plume and background, when compared to the same observations from actual field data, will provide a separate constraint on the range of reasonable biodegradation rates.

E-4.3. Methods

E-4.3.1. Data Collection and Preliminary Screening

Groundwater quality data were available from six LUFT sites located at existing and former military bases in California (Table E-4.1). These include the, the Area 43 Gas Station at Camp Pendleton Marine Corps Base (PMCB), the Petroleum, Oils, and Lubricants Fuel Farm Area at Castle Air Force Base (CAFB) near Merced, the Operable Unit #32 area at George Air Force Base (GAFB) near Victorville, the Building 637 area at the Presidio of San Francisco (PSF), the North-South Gas Station at Travis Air Force Base (TAFB) near Fairfield, and the Base Exchange Service Station at Vandenberg Air Force Base (VAFB) near Lompoc. Data included total petroleum hydrocarbons (TPH) and benzene/toluene/ethylbenzene/xylenes (BTEX), measured by gas chromatography. In addition, geochemical indicator parameters of hydrocarbon biodegradation processes were also measured, typically by ion chromatography or atomic adsorption spectroscopy. These include electron acceptors (dissolved oxygen, nitrate, sulfate) which may be consumed during biodegradation (Borden et al., 1995), ferrous iron and manganese which are mobilized when oxidized forms of these metals in oxyhydroxide minerals are used as electron acceptors (Lovley et al., 1989), and bicarbonate alkalinity and methane as biodegradation products. However, not all of the geochemical indicator data were available from all the sites.

Median values of geochemical parameter values at each of the six sites are shown on Table E-4.2. Interior wells were defined at each site as those wells containing TPH above the applicable detection limit; remaining wells were defined as background wells. Median values, as opposed to mean values, were chosen as representative values from the two categories to minimize the influence of extreme values. Concentration differences in geochemical indicators in plume wells and in background wells can be used to quantitatively compare electron acceptor utilization processes through reaction stoichiometry:



For almost every parameter at every site, differences in median values are consistent with biodegradation. Among the six sites as a whole, sulfate reduction appears to be the dominant process. If the magnitude of a geochemical indicator signature is defined as,

$$\Delta C = C_{plume}^* - C_{bkg}^* \quad (E-4-7)$$

where C_{plume}^* and C_{bkg}^* refer to the respective median plume interior and median background concentrations, then an inverse relationship should exist between Δc defined with respect to bicarbonate alkalinity (an expected positive value) and Δc defined with respect sulfate (an expected negative value). The relationship between Δc -bicarbonate alkalinity and Δc -sulfate for the six sites, based on Table E-4.2, is shown on Figure E-4.1, along with the ideal Δc relationship if sulfate reduction (Eq. E-4-5) were the only process affecting Δc -bicarbonate alkalinity. Given the approximate nature of the definition of Δc in Eq. E-4-7, the relationship between bicarbonate alkalinity and sulfate Δc values is compelling; the offset of the field estimates from the ideal relationship likely reflects the roles of other electron acceptors in influencing changes in bicarbonate alkalinity across the plumes. The internal consistency between bicarbonate alkalinity and sulfate geochemical indicators provides supporting evidence that bicarbonate alkalinity may be used to constrain the progress of biodegradation.

Plume lengths at the six sites were defined as the approximate distance from the source area to the downgradient edge of the TPH plume at the 10 parts-per-billion (ppb) contour level. Estimated plume lengths, based on two-dimensional TPH contour maps for each site, are shown on Table E-4.3.

E-4.3.2. Modeling Approach

Wilson and Miller (1978) presented an analytical solution for solute transport in a homogeneous, infinite aquifer of constant thickness with a uniform fluid flow field, assuming an instantaneous point source. When integrated over time, the source term is transformed into one of continuous mass injection,

$$c(x, y, t) = \int_{\tau=0}^{\tau=t} \frac{M_f}{4\pi\phi\tau H\sqrt{D_l D_t}} \exp\left[-\frac{(x-v\tau)^2}{4D_l\tau} - \frac{y^2}{4D_t\tau} - \lambda\tau\right] d\tau \quad (E-4-8)$$

where M_f is the mass introduced per unit time, ϕ the porosity, H the aquifer thickness, D_l and D_t the respective longitudinal and transverse dispersion coefficients, v the ground water velocity, λ the first-order decay coefficient, x and y , the spatial coordinates relative to the source location, and t the elapsed time between source introduction and sampling time. Given a set of values for the governing parameters in Eq. E-4-8, TPH concentrations may be predicted as a function of space and time. Plume length may be quantified along the longitudinal plume axis by setting $y = 0$ and solving for x , where c equals some prescribed concentration, using a search algorithm (e.g., bisection, Newton's method).

At (x, y) , the cumulative quantity of dissolved hydrocarbons which have undergone biodegradation, Δd , is given by superposition according to,

$$\Delta d(x, y, t) = \int_{\tau=0}^{\tau=t} \frac{M_f}{4\pi\phi\tau H\sqrt{D_l D_t}} \exp\left[-\frac{(x-v\tau)^2}{4D_l\tau} - \frac{y^2}{4D_t\tau}\right] d\tau - \int_{\tau=0}^{\tau=t} \frac{M_f}{4\pi\phi\tau H\sqrt{D_l D_t}} \exp\left[-\frac{(x-v\tau)^2}{4D_l\tau} - \frac{y^2}{4D_t\tau} - \lambda\tau\right] d\tau \quad (\text{E-4-9})$$

The generation of excess bicarbonate alkalinity over background may be estimated at any (x, y) by assuming a surrogate hydrocarbon compound such as toluene, C_7H_8 , represents the soluble, potentially biodegradable fraction of hydrocarbon which is measured as TPH at a given site. A value for Δc -bicarbonate alkalinity may then be defined in a manner analogous to the field data definition (Eq. E-4-6) by populating the spatial domain associated with each plume with a random distribution of monitoring wells.

At any given site, the representative values of the parameters in Eq. E-4-8 and Eq. E-4-9 that produce the most accurate model of the hydrocarbon plume and bicarbonate alkalinity plumes are generally unknown. However, field data and practical judgment may be used to place constraints on these values in the form of probability distribution functions. These probability distributions may be then be used in Monte Carlo simulations to generate multiple data sets representing a large number of idealized plumes. Specific simulation output consists of a set of plume lengths and associated Δc -bicarbonate alkalinity values characteristic of the synthetic plume population.

Probability distribution functions for the governing parameters in Eq. E-4-8 and Eq. E-4-9 are listed on Table E-4.4. A total of 500 Monte Carlo realizations were generated from these distributions using the Crystal Ball add-in package for Microsoft Excel (Decisioneering, Inc., 1996). A stand-alone computer program was written to calculate plume lengths and Δc -bicarbonate alkalinity values (using five to fifteen fictitious monitoring wells placed at random locations in the vicinity of each plume).

E-4.4. Results and Discussion

Rank-based correlation coefficients illustrating the relationships between model output (plume length and Δc -bicarbonate alkalinity) and input parameters are given on Table E-4.4. Among the input parameters and the associated probability distributions, variance in groundwater velocity and the biodegradation rate appear to largely control the variance in either model output. In retrospect, therefore, the choices of probability distributions for the other parameters (source term, aquifer thickness, dispersivity, age of plume) do not seem to be especially critical for the purposes of these simulations.

Inverse correlation characterizes the relationship between Δc -bicarbonate alkalinity and plume length (defined by the 10 ppb contour) among the synthetic plume population (Figure E-4.2). Intuitively, this is expected since low biodegradation rates tend to produce longer plumes and low Δc -bicarbonate alkalinity values, whereas the opposite is expected for high biodegradation rates (the extreme values present at either end of the graph reflect unrealistic biodegradation rates, coupled with particular chance combinations of the other variables). The relationship between these two plume metrics for the six field sites are also shown. The field observations are in generally good agreement with the synthetic plume metrics. The notable exception is the plume associated with the PMCB site, which appears to be too short given the observed Δc -bicarbonate

alkalinity value. However, this plume is truncated by discharge into a creek approximately 30 m downgradient from the source area. In the absence of the creek, the plume would be expected to extend further and thus would plot more toward the centerline shown on Figure E-4.2.

The forecast relationship between the biodegradation rate, λ , and Δc -*bicarbonate alkalinity* is shown on Figure E-4.3. An overall positive trend is apparent in the forecasts, although a great deal of scatter exists in the relationship (Table E-4.4). Assuming a lognormal distribution of Δc -*bicarbonate alkalinity* among the field data collected from the six sites, the values bracketed by one standard deviation range from 67 mg/L to 215 mg/L. The corresponding range of λ -values (bracketed by one standard deviation) falls between 4×10^{-4} and $7 \times 10^{-3} \text{ day}^{-1}$, with a geometric mean of $1.6 \times 10^{-3} \text{ day}^{-1}$. According to the model, lambda values above or below this interval would generally produce plumes with Δc -*bicarbonate alkalinity* values that would fall outside of those commonly observed in the field.

By itself, this constraint on lambda-values is tenuous because of the many simplifying assumptions in the model and the definition of Δc -*bicarbonate alkalinity* itself. However, plume length serves as an additional model output metric that can be used as an independent check on λ . The modeled relationship between λ and plume length is shown on Figure E-4.4. An overall negative trend is apparent in the forecasts, again with considerable scatter. Assuming a lognormal distribution of plume lengths for TPH among the six sites, the values bracketed by one standard deviation range from 56 m to 394 m. The corresponding range of λ -values (bracketed by one standard deviation) falls between 4×10^{-4} and $9 \times 10^{-3} \text{ day}^{-1}$, with a geometric mean value of $1.9 \times 10^{-3} \text{ day}^{-1}$.

Considering the broad simplifying assumptions inherent in the modeling, and the uncertainties in model parameters, the near-perfect agreement for the range of λ -values may well involve an element of chance. Nevertheless, the model does constrain the likely range of degradation rates to be on the order of 3×10^{-4} to $9 \times 10^{-3} \text{ day}^{-1}$ for the selected sites. Values of λ outside of this range would be expected to yield Δc -*bicarbonate alkalinities* and plume lengths that are not consistent with observation. Moreover, this range of values is consistent with first-order reaction rates estimated in other field studies. A review of published degradation rates estimated from field data under a variety of biogeochemical regimes (Table E-4.5) indicates a geometric mean value of $3 \times 10^{-3} \text{ day}^{-1}$, with a range encompassed by one standard deviation (lognormal distribution) of 4×10^{-4} to $3 \times 10^{-2} \text{ day}^{-1}$ (Figure E-4.5).

The mean biodegradation rates estimated by this study hold significant implications for remedial decision making. If rates of this order are supplied to Eq. E-4-8, along with median values from the probability distributions given on Table E-4.4, the analytical model predicts that such a plume would stabilize after only 10 to 15 years, no longer posing a threat to potential downgradient receptors. This prediction is actually conservative, given that the model assumes a source that is continuously active. When source removal activities occur, such as LUFT excavation and removal, such plumes would begin to decrease in size. These results may explain the recent empirical studies of Rice et al., 1995 and Mace et al., 1997, which indicated that the majority of existing LUFT-associated hydrocarbon plumes appear to be stable or declining under natural conditions, whereas only a small fraction appear to be experiencing further growth.

E-4.5. References

- Baedecker, M. J., I. M. Cozzarelli, R. P. Eganhouse, D. I. Siegel, and P. C. Bennett (1993), "Crude oil in a shallow sand and gravel aquifer **3**, Biogeochemical reactions and mass balance modeling in anoxic ground water," *Applied Geochemistry*, **8**(6) 569–586.
- Barker, J. F., G. C. Patrick, and D. Major (1987), "Natural attenuation of aromatic hydrocarbons in a shallow sand aquifer," *Ground Water Monitoring and Remediation*, Winter, 64–71.
- Borden, R. C., and P. B. Bedient (1986), "Transport of dissolved hydrocarbons influenced by oxygen-limited biodegradation **1**, Theoretical development, Water Resources Research, **22**(13), 1973–1982.
- Borden, R. C., C. A. Gomez, and M. T. Becker (1995), "Geochemical indicators of intrinsic bioremediation," *Ground Water*, **33**(2), 180–189.
- Borden, R. C., R. A. Daniel, L. E. LeBrun, C. W. Davis (1997), "Intrinsic biodegradation of MTBE and BTEX in a gasoline-contaminated aquifer," *Water Resources Research*, **33**(5), 1105–1115.
- Buscheck, T. E., and C. M. Alcantar (1995), "Regressive techniques and analytical solutions to demonstrate intrinsic bioremediation," in *Intrinsic Bioremediation*, R. E. Hinchee, J. T. Wilson, and D. Downey, Eds. (Battelle Press, Columbus, Ohio) pp. 109–116.
- Buscheck, T. E., D. C. Wickland, and D. L. Kuehne (1996), "Multiple lines of evidence to demonstrate natural attenuation of petroleum hydrocarbons, in *Proceedings from the Conference on Petroleum Hydrocarbons and Organic Chemicals in Ground Water*," National Ground Water Association/API, Houston, Texas, November 13–15.
- Chapelle, F. H., P. M. Bradley, D. R. Lovley, and D. A. Vroblesky (1996), "Measuring rates of biodegradation in a contaminated aquifer using field and laboratory methods," *Ground Water* **34**(4), 691–698.
- Cozzarelli, I. M., R. P. Eganhouse, and M. J. Baedecker (1990), "Transformation of monoaromatic hydrocarbons to organic acids in anoxic groundwater environment," *Environmental Geology and Water Science*, **16**(2), 135–141.
- Decisioneering, Inc. (1996), *Crystal Ball: Forecasting and Risk Analysis for Spreadsheet Users*. Decisioneering, Inc., Aurora, Colorado.
- Drever, J. I., (1988), "The Geochemistry of Natural Waters" (Prentice-Hall, Englewood Cliffs, New Jersey), 437 p.
- H_{ner}, A., P. H_{hener}, and J. Zeyer (1997), "Degradation of trimethylbenzene isomers by an enrichment culture under N₂O-reducing conditions," *Applied and Environmental Microbiology*, **63**(3), 1171–1174.
- Kazumi, J., M. E. Caldwell, J. M. Suflita, D. R. Lovley, and L. Y. Young (1997), "Anaerobic degradation of benzene in diverse anoxic environments," *Environmental Science and Technology*, **31**(3), 813–818.

- Lovley, D. R., M. J. Baedeker, D. J. Lonergan, I. M. Cozzarelli, E. J. P. Phillips, and D. I. Siegel (1989), "Oxidation of aromatic contaminants coupled to microbial iron reduction," *Nature*, **339**(5), 297–300.
- Lovley, D. R., J. D. Coates, J. C. Woodward, and E. J. P. Phillips (1995), "Benzene oxidation coupled to sulfate reduction," *Applied and Environmental Microbiology*, **61**(3), 953–958.
- Mace, R. E., R. S. Fisher, D. M. Welch, and S. P. Parra (1997), "Extent, Mass, and Duration of Hydrocarbon Petroleum Storage Tank Sites in Texas," *Bureau of Economic Geology*, University of Texas at Austin.
- Major, D. W., C. I. Mayfield, and J. F. Barker (1988), "Biotransformation of benzene by denitrification in aquifer sand," *Ground Water*, **26**(1), 8–14.
- McNab, W. W., Jr., and B. P. Dooher (1998), "Uncertainty analyses of fuel hydrocarbon biodegradation signatures in ground water by probabilistic modeling," *Ground Water*, **36**(4), 691–698.
- Reinhard, M., N. L. Goodman, and J. F. Barker (1984), "Occurrence and distribution of organic chemicals in two landfill leachate plumes," *Environmental Science and Technology*, **18**(12), 953–961.
- Rice, D. W., R. D. Grose, J. C. Michaelson, B. P. Dooher, D. H. MacQueen, S. J. Cullen, W. E. Kastenbergh, L. E. Everett, and M. A. Marino (1995), *California Leaking Underground Fuel Tank (LUFT) Historical Case Analyses*, Lawrence Livermore National Laboratory, Livermore, Calif. (UCRL-AR-122207).
- Rifai, H. S., R. C. Borden, J. T. Wilson, and C. H. Ward (1995), "Intrinsic bioattenuation for subsurface restoration," in *Intrinsic Bioremediation*, Hinchee, R. E., J. T. Wilson, and D. C. Downey, Eds. (Battelle Press, Columbus, Ohio), pp. 1–29.
- Salanitro, J. P. (1993), "The role of bioattenuation in the management of aromatic hydrocarbon plumes in aquifers," *Ground Water Monitoring and Remediation*, Fall, 150–161.
- Vroblesky, D. A., and F. H. Chapelle (1994), "Temporal and spatial changes of terminal electron-accepting processes in a petroleum hydrocarbon-contaminated aquifer and the significance for contaminant biodegradation," *Water Resources Research*, **30**(5), 1561–1570.
- Wiedemeier, T. H., et al. (1995), "Patterns of intrinsic bioremediation at two US Air Force Bases," in *Battelle Institute Proceedings of the Third Bioremediation Conference*, Hinchee, R. E., J. T. Wilson, and D. C. Downey, Eds., **3**(1), 32–51.
- Wiedemeier, T. H., M. A. Swanson, J. T. Wilson, D. H. Kampbell and others (1996), "Approximation of biodegradation rate constants for monoaromatic hydrocarbons (BTEX) in ground water," *Ground Water Monitoring and Remediation*, Summer, **16**(3), 186–194.
- Wilson, B. H., J. T. Wilson, D. H. Kampbell, B. E. Bledsoe, and J. M. Armstrong (1990), "Biotransformation of monoaromatic and chlorinated hydrocarbons at an aviation gasoline spill site," *Geomicrobiology*, **8**(3/4), 225–40.
- Wilson, B. H., J. T. Wilson, and D. Luce (1996), "Design and interpretation of microcosm studies for chlorinated compounds," in *Symposium on Natural Attenuation of Chlorinated Organics in Ground Water*, Dallas, Texas, September 11–13 (EPA/540/R-96/509), pp. 21–28.

- Wilson, J. L., and P. G. Miller (1978), "Two-dimensional plume in uniform ground-water flow," *Journal of the Hydraulics Division*, in *Proceedings of the American Society of Civil Engineers*, **104**(4), pp. 503–514.
- Wilson, J. T., D. H. Kampbell, and J. Armstrong (1994), "Natural bioreclamation of alkylbenzenes (BTEX) from a gasoline spill in methanogenic groundwater," in *Hydrocarbon Bioremediation*, Hinchee, R. E., B. C. Alleman, R. E. Hoeppe, and R. N. Miller, Eds. (Lewis Publishers, Boca Raton, Florida), pp. 201–218.
- Wilson, J. T., G. Sewell, D. Caron, G. Doyle, and R. N. Miller (1995), "Intrinsic Bioremediation of Jet Fuel Contamination at George Air Force Base," in *Intrinsic Bioremediation*, Hinchee, R. E., J. T. Wilson, and D. C. Downey, Eds. (Battelle Press, Richland, Washington), pp. 91–100.

Table E-4.1. Sites included in study.

LUFT site location	Hydrogeologic setting	Contaminant	Number of monitoring wells	Analytes
Camp Pendleton Marine Corps Base (PMCB)	Coastal canyon alluvium and fill	Gasoline	16	TPH, BTEX, HCO ₃ ⁻ (as alkalinity), CH ₄ , Eh, Fe ²⁺ , O ₂ , NO ₃ ⁻ , pH, SO ₄ ²⁻
Castle Air Force Base (CAFB)	Broad alluvial plain	Aviation fuel (JP-4)	19	TPH, BTEX, HCO ₃ ⁻ (as alkalinity), CH ₄ , Eh, Fe ²⁺ , Mn ²⁺ , O ₂ , NO ₃ ⁻ , pH, SO ₄ ²⁻
George Air Force Base (GAFB)	High desert alluvial fan	Aviation fuel (JP-4)	16	TPH, BTEX, HCO ₃ ⁻ (as alkalinity), CH ₄ , Eh, Fe ²⁺ , Mn ²⁺ , O ₂ , NO ₃ ⁻ , pH, SO ₄ ²⁻
Presidio of San Francisco (PSF)	Shallow marine deposits, organic-rich	Gasoline and diesel	13	TPH, BTEX, HCO ₃ ⁻ (as alkalinity), CH ₄ , Eh, Fe ²⁺ , Mn ²⁺ , O ₂ , NO ₃ ⁻ , pH, SO ₄ ²⁻
Travis Air Force Base (TAFB)	Broad alluvial plain	Gasoline	29	TPH, BTEX, HCO ₃ ⁻ (as alkalinity), CH ₄ , Eh, Fe ²⁺ , Mn ²⁺ , O ₂ , NO ₃ ⁻ , pH, SO ₄ ²⁻
Vandenberg Air Force Base (VAFB)	Shallow marine deposits	Gasoline	14	TPH, BTEX, HCO ₃ ⁻ (as alkalinity), CH ₄ , Eh, Fe ²⁺ , Mn ²⁺ , NO ₃ ⁻ , pH, SO ₄ ²⁻

Table E-4.2. LUFT site geochemical indicator data (concentrations given in mg/L).

Species	Zone	PMCB	CAFB	GAFB	PSF	TAFB	VAFB
O ₂	Plume	0.65	2.1	3.4	0.4	0.2	* n.a.
	Background	1	2.9	6.4	0.3	0.5	n.a.
	Δc	-0.35	-0.8	-3.0	0.1	-0.3	n.a.
NO ₃ ⁻	Plume	1.6	2.8	0.3	0.01	0.3	0.05
	Background	3.2	6.5	1.4	0.06	5.5	0.07
	Δc	-1.6	-3.7	-1.1	-0.05	-5.2	-0.02
SO ₄ ²⁻	Plume	70.4	15.9	53	10.2	456	3.9
	Background	84	27.1	137.5	48.3	740	200
	Δc	-13.6	-11.2	-84.5	-38.1	-284	-196.1
Fe ²⁺	Plume	1.5	0.05	0.05	4.7	2.97	3.3
	Background	0	0.007	0	0.03	0.02	0.8
	Δc	1.5	0.043	0.05	4.67	2.95	2.5
Mn ²⁺	Plume	n.a.	0.88	1.5	0.78	2.9	0.50
	Background	n.a.	0.5	0	0.43	0.2	0.22
	Δc	n.a.	0.38	1.5	0.35	2.7	0.28
†HCO ₃ ⁻	Plume	466	262	252	500	621	500
	Background	393	182	176	383	327	300
	Δc	73	80	76	117	294	200
CH ₄	Plume	0.9	0.006	0.002	7	0.21	0.26
	Background	0.006	0.0006	0.0002	0.3	0.005	0.004
	Δc	0.9	0.0054	0.0018	6.7	0.205	0.256

Table E-4.3. Inferred TPH plume lengths, as defined by the 10 part-per-billion contour line.

Site	Plume length (m)
PMCB	30
CAFB	210
GAFB	610
PSF	180
TAFB	120
VAFB	120

* n.a. = data not available.

† Reported as bicarbonate alkalinity.

Table E-4.4. Probability distributions used in Monte Carlo realizations.

Parameter	Probability distribution ¹	Basis	R (Plume length)	R(calc)
Source term (Mf)	18,900 - 151,400 liters	Postulated.	0.08	0.09
Aquifer thickness (H) ²	4.6 - 15 m	Site hydrostratigraphies.	-0.04	-0.13
Groundwater velocity (v)	0.003 - 1.0 m/day	Estimated mean hydraulic conductivities by pumping tests; interpolated mean hydraulic gradient, Darcy's law.	0.68	-0.69
Degradation coefficient (λ)	0.01% - 2% day ⁻¹	Postulated based on commonly reported range in the literature.	-0.57	0.35
L:L ratio ³	0.03 - 0.33	Assumed dispersivity to plume length scale ratio.	0.13	-0.02
T:L ratio	0.003 - 0.03	Assumed dispersivity to plume length scale ratio.	-0.03	-0.11
Elapsed time since source initiation (t) ⁴	20 - 40 years	Site histories.	0.09	-0.12

¹As defined by the applicable analytical detection limit, typically equal to or less than 1 µg/L.

²Includes wells sampled as part of site natural attenuation assessment; does not include all monitoring wells at each site.

³Considered only when detected in five or more wells.

⁴Best-fit between normal and lognormal distributions determined by the Kolmogorov-Smirnov test.

Table E-4.5. Selected published reaction rates for benzene estimated from field data at groundwater contamination sites.

Conditions	Rate (day ⁻¹)	Reference
Iron-reducing	1.1×10^{-4}	<i>Wilson et al. (1996)</i>
Iron-reducing	2.0×10^{-4}	<i>Rifai et al. (1995)</i>
Nitrate-reducing, sulfate-reducing, and methanogenic	4.3×10^{-4}	<i>Wilson et al. (1994)</i>
Nitrate-reducing	9.0×10^{-4}	<i>Borden et al. (1997)</i>
Iron-reducing	2.2×10^{-3}	<i>Wilson et al. (1996)</i>
Methanogenic	7.1×10^{-3}	<i>Wilson et al. (1990)</i>
Sulfate-reducing	1.8×10^{-2}	<i>Wiedemeier et al. (1995)</i>
Methanogenic	1×10^{-2}	<i>Wiedemeier et al. (1995)</i>
Methanogenic, iron-reducing, manganese-reducing	1.7×10^{-2}	<i>Cozzarelli et al. (1990)</i>
Sulfate-reducing	2.8×10^{-2}	<i>Wiedemeier et al. (1996)</i>
Sulfate-reducing	3.8×10^{-2}	<i>Wiedemeier et al. (1996)</i>

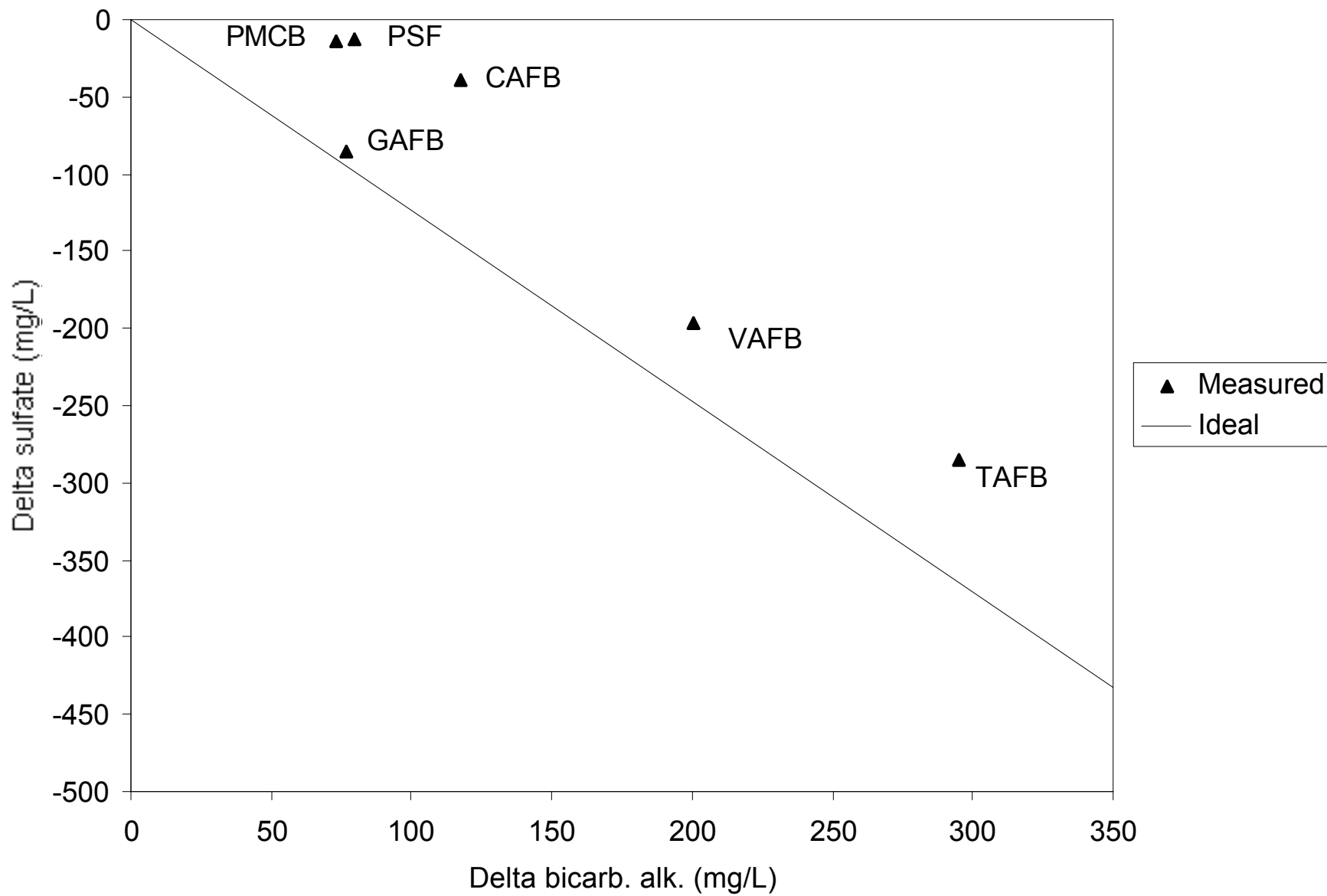


Figure E-4.1. Relationship between Δc -sulfate and Δc -bicarbonate alkalinity.

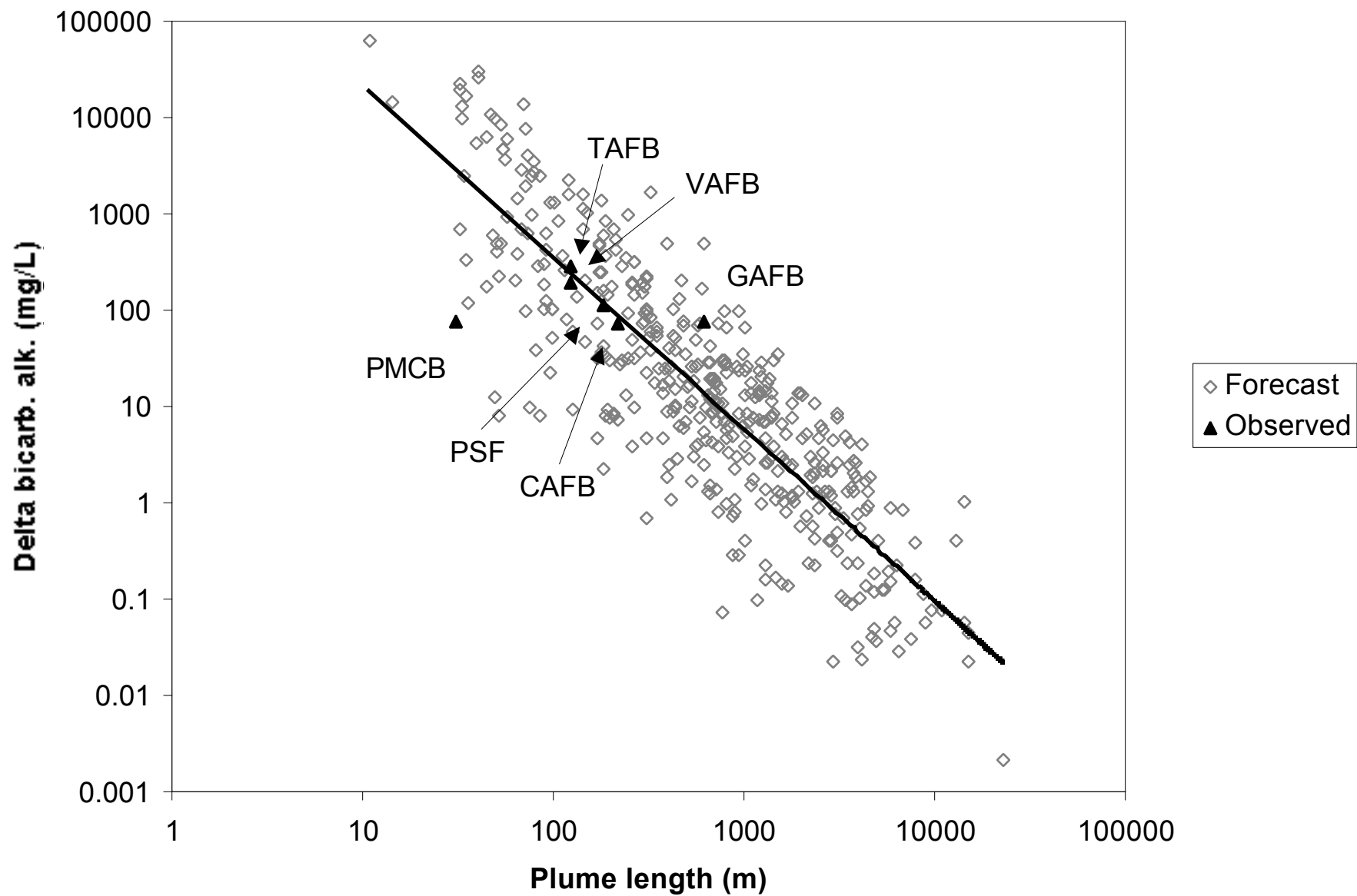


Figure E-4.2. Relationship between plume length and Δc -bicarbonate alkalinity for Monte Carlo realizations (forecast synthetic plumes) and field data.

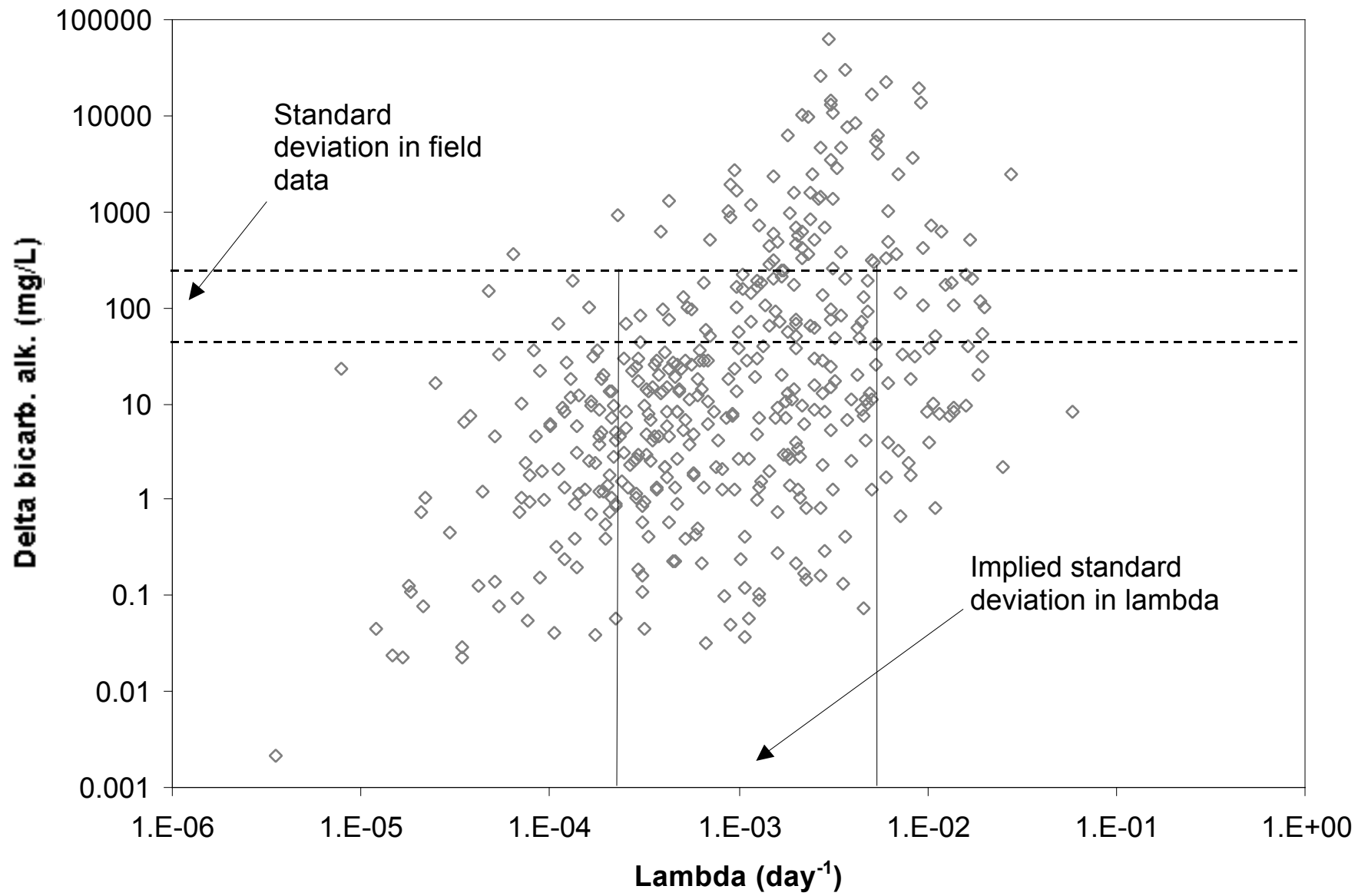


Figure E-4.3. Relationship between Δc -bicarbonate alkalinity and degradation rate (λ) in forecast synthetic plumes.

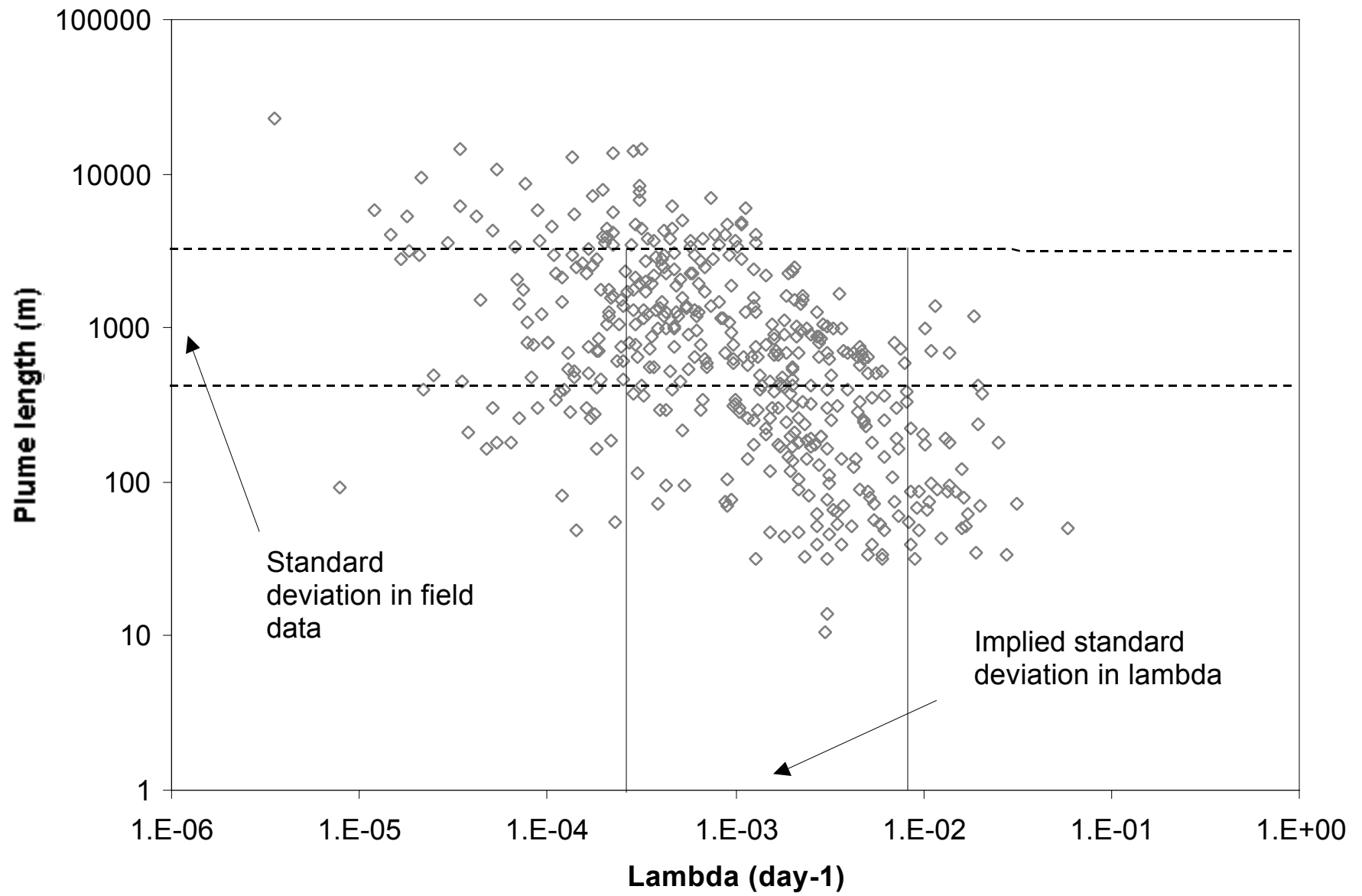


Figure E-4.4. Relationship between plume length and degradation rate (λ) in forecast synthetic plumes.

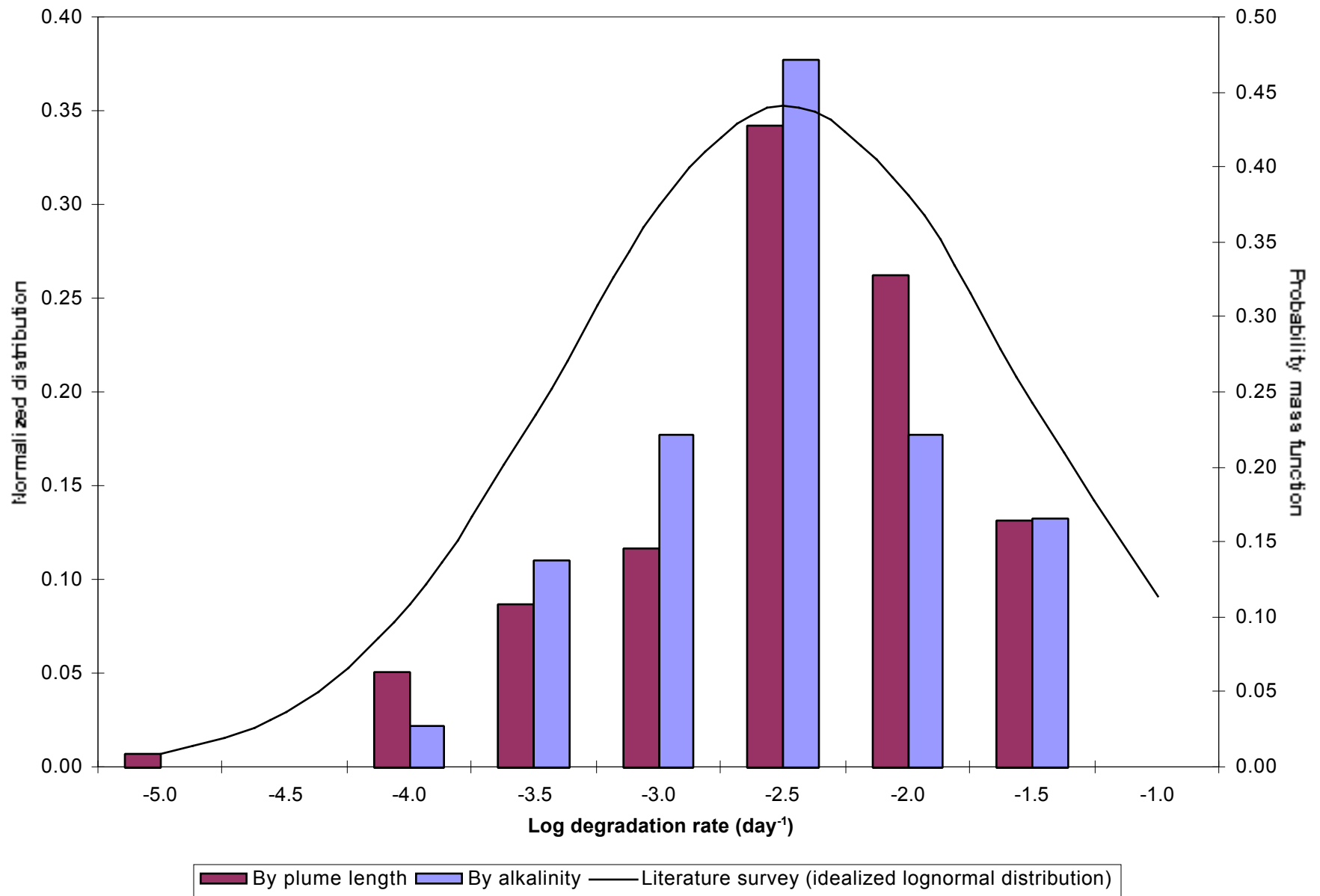


Figure E-4.5. Probability distributions of degradation rates; literature (for benzene) and this study (for TPH as gasoline).